university of groningen / faculty of science and engineering

Habitability of Earth-like Exoplanets Around Low-mass Stars

Erika Giorgi, s3628582

Astronomy Bachelor Thesis

Primary Supervisor: Prof. Dr. Inga Kamp
Secondary Supervisor: Mark Oosterloo

July 2, 2021

Acknowledgements

I would like to thank my two supervisors, Prof. Dr. Inga Kamp and Mark Oosterloo for their continuous enthusiasm and incredibly helpful guidance throughout the work of this thesis. I very much appreciate your patience in taking the time to explain the planetary evolution and carbon cycle model and helping me through the programming aspects of this work.

Abstract

Context: Some of the most promising candidate systems to find extraterrestrial life are low-mass stars for their relative abundance in the Milky Way and long evolutionary timescales. Habitability is defined in terms of the possible presence of liquid water, and thus temperate climate conditions which can be regulated by the carbon cycle and greenhouse effect mechanisms, such as on Earth.

Aims: In this work, we aim to investigate whether habitable surface conditions can be sustained on an Earth-like exoplanet orbiting a low-mass ($0.1-1\,\mathrm{M}_\odot$) star of M-K spectral type, and compare these results to the Earth. The evolution of planetary surface temperature T_{surf} and atmospheric CO_2 pressure $P_{\mathrm{CO_2}}$ are studied up to 20 Gyr.

Methods: The luminosity evolution of the central star is determined from our generalized stellar evolution model using existing tables from Siess, Dufour, and Forestini (2000). The evolution of various carbon reservoirs (surface, crust and mantle) is modeled as a function of time to determine the long-term evolution of T_{surf} and $P_{\mathrm{CO_2}}$. The offset between stellar and planetary evolution is 1 Gyr, such that the planet is fully formed and the star is on the main sequence. We model the system for which a planet around stars of mass $0.1\,\mathrm{M}_\odot$ and $0.5\,\mathrm{M}_\odot$ receives the same stellar irradiance at $t = 0$ as the Earth does from the Sun. Subsequently, a range of five circumstellar distances are evaluated to determine the habitable limits for the same stellar masses. Finally, we apply the model to the system of Proxima Centauri b to evaluate possible long-term habitability.

Results: The Earth analogs around low-mass stars do not receive sufficient stellar irradiation at their respective distances to sustain habitable surface conditions in terms of T_{surf} and $P_{\mathrm{CO_2}}$, experiencing sub-freezing temperatures for Gyr timescales. For a $0.1\,\mathrm{M}_\odot$ star, the habitable zone lies between $0.023 - 0.029$ AU. The habitable range for a $0.5\,\mathrm{M}_\odot$ star is $0.180 - 0.220$ AU where the limits are imposed by the freezing point of water (273 K) and the degradation of proteins necessary for photosynthesis (343 K), with a lower limit of $P_{\mathrm{CO_2}} = 0.101$ Pa for habitability.

Conclusions: Habitable surface conditions are possible on Earth-like exoplanets orbiting low-mass stars for long periods of time. Stars of mass $\sim 0.1\,\mathrm{M}_\odot$ have very long main sequence lifetimes, and thus habitable conditions could be maintained for thousands of Gyr. $0.5\,\mathrm{M}_\odot$ stars have shorter evolutionary timescales with shorter main sequence lifetimes and thus the habitable zone limits can only be sustained for several tens of Gyr. The system of PCb has temperatures too low to support life.

Contents

1 Introduction

1.1 Exoplanet Occurrence

In the observable Universe there are hundreds of billions of galaxies, each with several hundred billion stars (Perryman, 2018). In the Milky Way alone, it has been estimated that there are 100 billion planets, 6 billion of which are Earth-like, and 300 million are deemed to be potentially habitable considering the host star's habitable zone (Safonova et al., 2021). It is therefore inevitable to ask ourselves the question if planetary systems such as our own exist somewhere else, and if so, can they harbor intelligent life? The research field of extraterrestrial systems has been evolving and expanding rapidly since the late 1980s with the first results of sub-stellar companions around stars similar to our Sun (Perryman, 2018). However, the most common type of star in our galaxy, and throughout the Universe, is the M dwarf (also known as a red-dwarf) (Adams, Bodenheimer, and Laughlin, 2005). In fact, 75% of the main sequence stars in the Milky Way are characterized as M-dwarfs (Safonova et al., 2021). Their low mass (less than one solar mass) means that any changes in the observed radial velocity profile by an orbiting planet are more pronounced than for larger G-K type stars (Perryman, 2018).

Planets around these types of low-mass stars are believed to be common, as demonstrated by Gaidos et al. (2016) with the result that on average, there are 2.2 ± 0.3 planets with radii $1 - 4\,\mathrm{R}_\oplus$ (where $R_\oplus$ is the radius of the Earth) around M dwarfs (detected by the Kepler space telescope). Many planets have been determined to be Earth-like, meaning they are rocky and of similar size and composition to the Earth. An Earth-like planet should ideally be within the range $0.5 - 1.4\,\mathrm{M}_\oplus$ (where $\mathrm{M}_\oplus$ is the mass of the Earth) for possible similarity of interior and atmospheric processes (Kopparapu, 2013). As such, these types of terrestrial planets around these low-mass stars occur very frequently, twice as much as for G-type stars such as the Sun (Perryman, 2018). For this reason, they are considered some of the most probable candidates for finding extraterrestrial life. However, there is still limited knowledge about specific properties of these planets from observations, such as their atmospheric or surface structure and composition.

1.2 Habitable Zone Conditions

The definition of a habitable zone is generally accepted to be the region around a star where water can be sustained in a stable liquid form over geologic timescales (more than 10 Myr) (Perryman, 2018). The presence of liquid water on a planet is thought to be a necessary prerequisite for the existence of known carbon-based life, as it is necessary to support self-sustaining chemical reactions (Perryman, 2018). Therefore, this condition of liquid water sets a boundary for the potential habitability of exoplanets in different stellar systems.

The habitable region is mostly determined by the mass M, effective temperature T_{eff}, and

corresponding luminosity L of the star. For our Sun, a G2V type star currently on the main sequence with $T_{\text{eff}} \sim 5778\,\text{K}$, this means a habitable zone of $0.9 - 1.5\,\text{AU}$ determined by the solar irradiation necessary to sustain liquid water (Lissauer, 2018). However, the surface temperature of a planet is not the only factor that can determine whether liquid water is present or not, as it also depends on atmospheric pressure (Pierrehumbert, 2009). For example, it is possible for water to exist in a stable liquid form even for temperatures higher than 500 K, with sufficient pressure provided by atmospheric water vapor (Pierrehumbert, 2009).

1.2.1 Our position in the habitable zone

The Earth is situated at the inner edge of the Sun's habitable zone, at a distance of one astronomical unit (AU). The short-wave stellar irradiation from the Sun reaches the surface and is partially reflected back into the atmosphere as infrared radiation. Greenhouse gases such as water vapor (H_2O) and carbon dioxide (CO_2) in the atmosphere absorb and re-emit most of this infrared emission back towards the Earth's surface (Pierrehumbert, 2009). These gases allow for the solar radiation to pass through almost unimpeded, but block a large part of the outgoing infrared radiation, increasing the Earth's average surface temperature (Pierrehumbert, 2009). Therefore, more greenhouse gases in the atmosphere result in more heat trapped, increasing the temperature on Earth.

A surface temperature range of $273 - 343\,\text{K}$ is considered the standard metric for the survival of life based on Earth's history. This temperature range has been present on Earth for the past $\sim 4\,\text{Gyr}$, from periods of much lower solar luminosity at initial stages of the Sun's evolution on the main sequence (Rushby et al., 2018). Beyond temperatures of 343 K, most species cannot survive due to a degradation of proteins necessary for photosynthesis (Rushby et al., 2018). This temperature range excludes extremophile species which have been observed to withstand temperatures of $253 - 395\,\text{K}$ (Rushby et al., 2018). As the Sun evolves on the main sequence, it will steadily increase in luminosity, eventually becoming a red giant at $\sim 10\,\text{Gyr}$ (5.5 Gyr from the present-day). In turn, the habitability of the Earth becomes irrelevant to consider past this stage due to the extreme high temperatures (LeBlanc, 2011). This can be explained in terms of the 'runaway greenhouse' effect. In this case, the higher surface temperatures result in increased amounts of water vapor entering the atmosphere by evaporation, increasing the greenhouse effect and leading to even higher surface temperatures. This positive feedback loop only terminates when there is no more surface liquid water to evaporate, in a timescale of $\sim 1\,\text{Gyr}$, by which point the planet is no longer considered habitable (Pierrehumbert, 2009; Wolf et al., 2017). This limit occurs for $T_{\text{surf}} \gtrsim 355\,\text{K}$, but the planet can be considered uninhabitable to most species already before this limit (Wolf et al., 2017). Beyond the outer edge of the habitable zone, a 'runaway ice-house' or 'maximum CO_2 greenhouse' effect would occur. Here, all surface water can become frozen in a few thousand years as the greenhouse warming mechanism is not effective enough in sustaining a temperate climate due to high levels of CO_2 condensation and an increase in Rayleigh scattering (Lehmer, Catling, and Krissansen-Totton, 2020; Pierrehumbert, 2009).

In Figure 1, the various habitable zone distances based on the runaway greenhouse and maximum CO_2 greenhouse effects, represented by the inner and outer blue lines respectively, are shown for main sequence stars of mass $0.1-1\,M_\odot$ where $M_\odot$ is the current mass of the Sun. These habitable zone boundaries are fixed for a particular star on the main sequence. The solar system planets, along with several detected exoplanets located in their star's habitable zone, such as Proxima Centauri b, are also shown for reference.

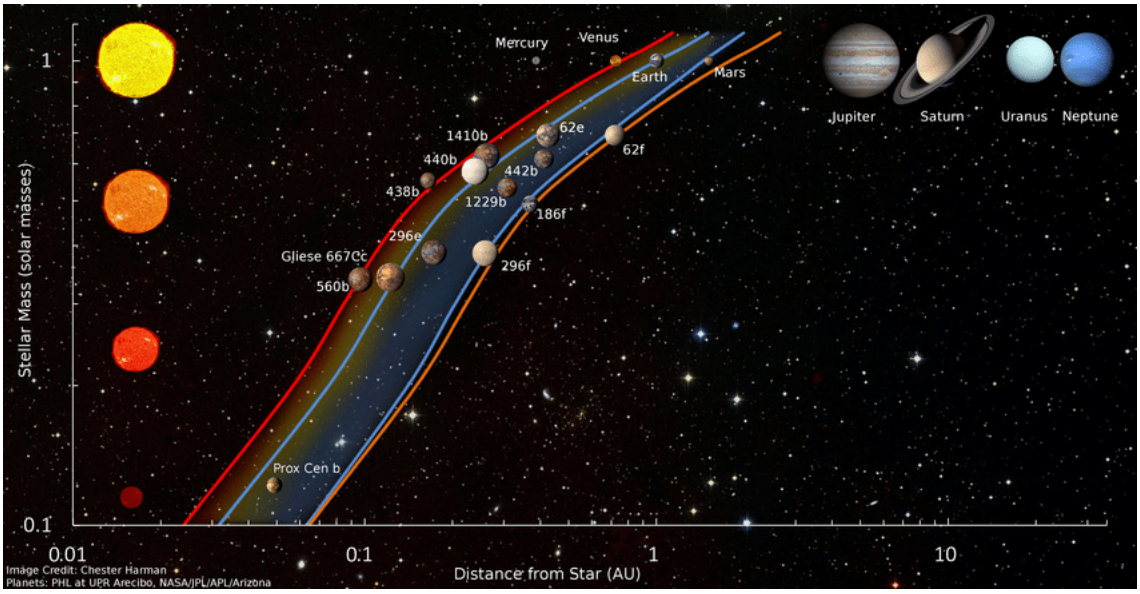

Figure 1: Habitable zone limits for main sequence stars of mass $0.1 - 1\,M_\odot$, determined by the runaway greenhouse and maximum CO_2 greenhouse effects, indicated by the inner and outer blue lines respectively. The 'recent Venus' (inner red line) and the 'early Mars' (outer orange line) are also shown, along with the solar system planets and several detected exoplanets for reference. Image source: Shields, Ballard, and Johnson (2016). Image credit: Chester Harman.

Also depicted in Figure 1 are the two scenarios for the 'recent Venus' (inner red line) and the 'early Mars' (outer orange line) which are representative of more optimistic habitable zone limits from studies of Kopparapu (2013). The first is from the suggestion that liquid water has not been present on the surface of Venus for at least 1 Gyr, at which time the Sun's luminosity was $0.92L_\odot$, where $L_\odot$ is the current value of the solar luminosity. These studies provide an empirical estimate for the present-day inner edge of the Sun's habitable zone of 0.75 AU. The second scenario (early Mars) is based on the assumption that the red planet's surface temperatures could have allowed for liquid water to be sustained ~ 3.8 Gyr ago (Kopparapu, 2013). At this time, the Sun's luminosity was $\sim 0.75\,L_\odot$, thus setting the empirical estimate for the present-day habitable zone at 1.77 AU (Kopparapu, 2013). Overall, Figure 1 allows us to visualize the extent of habitable zone differences, not just for a solar type star, but also stars of lower mass of which this work focuses on.

1.2.2 Habitable zone from planetary and stellar evolution

Stellar evolution plays a major role in the determination of a habitable zone for its orbiting planets. The lower luminosity of the Sun in the past would mean that the Earth should have been frozen over in these initial stages. This is known as the 'Faint Young Sun' problem (Lissauer, 2018). However, this contradicts geological evidence that a temperate climate has been present on Earth during that time of lower solar luminosity (Sleep and Zahnle, 2001). The solution to this problem is based on the abundant presence of greenhouse gases in the atmosphere, most notably CO_2 and H_2O (Lissauer, 2018). A planet's surface temperature is not only determined by exterior factors of the central star, but also interior mechanisms such as radiogenic heating in the mantle (Lissauer, 2018). Other processes which have an influence on surface temperature, but are not considered in further detail in this work are tidal heating, the albedo effect (or reflectivity), and the atmospheric or oceanic circulations (Lissauer, 2018).

Climate stabilizing mechanisms are considered necessary in maintaining habitable conditions over geologic timescales (Walker, Hays, and Kasting, 1981). On Earth, the carbon cycle has played an important role in stabilizing the climate for the past 3.5 Gyr during which life has been evolving (Perryman, 2018). It is believed that this balance between positive feedback of the greenhouse effect and the negative feedback from the correlation of CO_2 levels in the atmosphere and surface temperature can significantly alter the habitable zone boundaries (Perryman, 2018). Also known as the carbonate-silicate cycle due to the importance of silicate weathering, this equilibrium mechanism is thus important to consider for Earth-like exoplanets. In connection to the carbon cycle are plate tectonics, which could be a potential requirement for habitability on an Earth-like planet if stable surface temperatures are considered a prerequisite for the formation and evolution of life (Perryman, 2018). Even though the Earth is the only planet in the solar system with active plate tectonics, it is possible that rocky exoplanets with a similar size and composition as the Earth can have these properties, and thus climate stabilizing mechanisms to host life (Pierrehumbert, 2009). Even though significant progress has been made in the research field of exoplanets, habitability conditions are still a source of intense debate.

All in all, the surface temperature of a planet and the amount of CO_2 in the atmosphere can be two indicators for possible habitability, which we consider the two most important quantities to evaluate for a planet's long-term evolution.

1.3 Evolution of Low-mass Stars

Low-mass stars are the most abundant in our galaxy, it is therefore important to consider their exoplanets, if any, as prime candidates for finding possible extraterrestrial life. Understanding the stellar evolution can help to better estimate the potential habitability of their exoplanets. In this work, particular focus is placed on the lowest-mass stars ($0.1 - 1\,M_\odot$) for their relatively long main sequence lifetimes compared to the Sun. M-dwarfs are character-

ized by their very small mass, in the range $0.08 - 0.6\,M_\odot$, and low effective temperatures of $2500 - 3800\,K$ with faint luminosities of $0.0003 - 0.457\,L/L_\odot$ (Perryman, 2018; Scalo et al., 2007). Consequently, the habitable zone of any orbiting planets lies much closer to the star with respect to the Earth - Sun distance in order to sustain temperatures for liquid water (Perryman, 2018). However, several factors should be considered with regards to potential habitability of planets around these types of stars. Tidal locking effects can become significant with very small circumstellar distances, affecting the overall planetary surface evolution (Perryman, 2018). Also important are the potentially lethal stellar flares, most frequent and intense during the first billion years of the M-star's lifetime (Perryman, 2018). After this initial $\sim 1\,Gyr$ period, the star has settled onto the main sequence without experiencing significant changes in luminosity for several hundreds and even thousands of Gyr (Scalo et al., 2007). K-type stars are slightly warmer than M-type, with a temperature range of 3500-5000 K (LeBlanc, 2011). These types of main sequence stars are the second-most common in the galaxy. One reason for considering them as good candidates for habitable planets is due to their similarity in solar radiation output and stellar behaviour with respect to the Sun. Furthermore, unlike the M stars, these orange dwarfs are not expected to have as strong stellar flares, thus possibly providing more habitable conditions on nearby planets (LeBlanc, 2011).

The evolution of a star after its formation begins with the pre-main sequence phase, for which the star is fully convective and hydrogen fusion into helium has not yet begun (LeBlanc, 2011). The time that a star spends in this phase is dependent on its mass, with lower mass stars having longer evolutionary timescales (LeBlanc, 2011). The start of an extended phase of rather constant luminosity for such a low-mass star is the zero age main sequence (ZAMS), with the fusion of hydrogen in the stellar core (LeBlanc, 2011). Since low-mass stars burn their fuel at very slow rates due to being fully convective for large portions of their lives, their main sequence lifetimes are exceedingly long, much longer than the age of the Universe of 13.7 Gyr (LeBlanc, 2011). Stars of mass $M \lesssim 0.25\,M_\odot$ remain fully convective for their entire lifetimes, burning their hydrogen fuel at very slow rates (LeBlanc, 2011). None of these types of stars have evolved off of the main sequence yet, especially those of lowest mass whose lifetimes can extend to several trillions of years (LeBlanc, 2011). As stars steadily fuse hydrogen into helium, they increase in luminosity. In order to maintain an equilibrium, a star must either expand (as the Sun does towards the end of its main sequence, eventually evolving into a red giant), or increase in temperature to become a blue dwarf (for low-mass M-type stars) (Adams, Bodenheimer, and Laughlin, 2005). After this phase, having exhausted its fuel, a star generally evolves off of the main sequence, either becoming a red giant and then a white dwarf for a star such as the Sun, or evolving into a blue and eventually white dwarf as is the case for lower-mass stars of $M \lesssim 0.5\,M_\odot$ (Adams, Bodenheimer, and Laughlin, 2005).

For the case of the Sun, as the fusion process of hydrogen into helium takes place in the core, the mean molecular weight in this region increases (Christensen-Dalsgaard, 2021). This results in a core contraction, increasing the density, temperature and therefore luminosity. This increase in luminosity is significant for life on Earth, as surface temperatures will eventually rise past the habitable limit of 343 K. This is one of the main reasons for researching

and observing low-mass stars, as their longer evolutionary timescales do not present this increase in luminosity at such early stages as the Sun, and could thus benefit the long-term evolution and survival of life on their exoplanets.

The main sequence lifetime of a star, $t_{\rm MS}$, can be calculated from its mass M, by the following relation from Hansen and Kawaler (1994):

$$\frac{t_{\rm MS}}{t_\odot} \sim \left(\frac{M}{M_\odot}\right)^{-2.5}. \tag{1}$$

Here, $t_\odot$ is the main sequence lifetime of the Sun, 10 Gyr. From eq. (1), the values of $t_{\rm MS}$ for M- and K-type stars on the main sequence (denoted by the Roman numeral V) have been calculated and are presented in Table 1 (K-type) and Table 2 (M-type) below, with the stellar properties obtained from Mamajek (2021).

Type	$\mathbf{M/M_\odot}$	$\mathbf{L/L_\odot(\%)}$	$\mathbf{T_{eff}}$ **(K)**	$\mathbf{t_{MS}}$ **(Gyr)**
K0V	0.880	45.7	5270	13.766
K1V	0.860	40.7	5170	14.580
K2V	0.820	37.2	5100	16.424
K3V	0.780	28.2	4830	18.611
K4V	0.730	20.4	4600	21.963
K5V	0.700	17.4	4440	24.392
K6V	0.690	13.8	4300	25.286
K7V	0.640	10.0	4100	30.518
K8V	0.620	8.7	3990	33.039
K9V	0.590	7.9	3930	37.400

Table 1: K-type star spectral type, stellar mass (in solar units), percentage of solar luminosity, effective temperature (K) and main sequence lifetime (Gyr).

Type	$\mathbf{M/M_\odot}$	$\mathbf{L/L_\odot(\%)}$	$\mathbf{T_{eff}}$ **(K)**	$\mathbf{t_{MS}}$ **(Gyr)**
M0V	0.570	6.92	3850	40.767
M1V	0.500	4.07	3660	56.568
M2V	0.440	2.90	3470	77.879
M3V	0.370	1.62	3430	120.087
M4V	0.230	0.724	3210	394.167
M5V	0.162	0.302	3060	946.700
M6V	0.102	0.105	2810	3009.536
M7V	0.090	0.0646	2680	4115.226
M8V	0.085	0.0525	2570	4747.366
M9V	0.079	0.0302	2380	5700.754

Table 2: M-type star spectral type, stellar mass (in solar units), percentage of solar luminosity, effective temperature (K) and main sequence lifetime (Gyr).

One particular exoplanet and low-mass star system interesting to study is that of Proxima Centauri b (PCb) at a distance of 1.302 pc, making it the closest stellar neighbour to our Sun. The central star is classified as an M5.5V, with a mass of $0.12\,M_\odot$ and effective temperature of $\sim 3050\,K$ (Anglada-Escudé et al., 2016). Being a red dwarf, its luminosity is only 0.15% that of the Sun, and therefore the suggested habitable zone for planets lies very close to the star at $0.04 - 0.08\,AU$. The confirmed exoplanet orbiting at a distance of $\sim 0.05\,AU$ is considered to be within the habitable zone, receiving a stellar irradiance of 65% that of Earth (Anglada-Escudé et al., 2016). This system will be modeled and studied more closely in Section 4.3.

1.4 Planetary Structure and the Carbon Cycle

In order to understand the surface conditions of an Earth-like planet, its interior evolutionary processes must be taken into account as they can largely the influence the climate via processes such as plate tectonics necessary for the carbon cycle. Throughout this work, the term 'Earth-like' is used to mean a planet of exactly the same terrestrial composition as the fully-formed Earth. Firstly, a brief explanation of the carbon cycle is provided, as it is the principal climate regulating mechanism for the Earth over geologic timescales.

The interior of the Earth, and thus the Earth-like planets considered in this work, is composed of a core, mantle and crust. The upper layer of the mantle and crust compose the lithosphere, which make up the tectonic plates. Below is the asthenosphere, which can be considered a viscous fluid on geological timescales (Schubert, Turcotte, and Olson, 2001). The Earth's crust is composed of the thicker continental crust (average thickness of 35 km) and the denser, thinner oceanic crust (average thickness of 6 km). Due to the characteristics of the oceanic crust, certain regions are gravitationally unstable, causing the formation of a subduction zone in which the crust and lithosphere sink down into the mantle. The region where this occurs is known as a convergent plate boundary, and it is where most of the Earth's active volcanoes and tectonic activity occur. Through this subduction process, carbon from the surface of the Earth can be efficiently transported into the mantle of high viscosity. The mantle is heated internally from the decay of radioactive isotopes through the process known as radiogenic heating (Schubert, Turcotte, and Olson, 2001). This determines the mantle viscosity, which in turn affects the mean plate speed through convection.

The long-term carbon cycle provides the necessary negative feedback mechanism for the maintenance of habitable temperatures on Earth (conditions for liquid water as it is required for weathering reaction processes) by regulating the atmospheric CO_2 concentrations (Foley, 2015). CO_2 is removed from the atmosphere by silicate weathering occurring on the continental crust as the CO_2 reacts with rocks exposed to the atmosphere to form bicarbonate. The carbon is then deposited as carbonate rocks on ocean plates (Foley, 2015). The carbon cycle is water-mediated, and can thus only operate with surface liquid water for the CO_2 to dissolve into (James Kasting, Whitmire, and Reynolds, 1993). Eventually, the carbon is subducted at convergent plate boundaries, and is partially transported deep into the mantle, and partially returned to the atmosphere by processes such as metamorphic

degassing and arc volcanism (Foley, 2015). At mid-oceanic ridges, the carbon in the mantle degasses back into the atmosphere and oceans, which completes the carbon cycle (Foley, 2015).

This process is heavily dependent and interconnected with the planetary surface temperature, as higher temperatures increase the weathering rate, leading to more CO_2 being drawn out of the atmosphere and oceans (Foley, 2015). This has the effect of cooling, and thus stabilizing, the climate via a reduced greenhouse effect, since the degassing rate stays the same, to achieve an equilibrium (Foley, 2015). Similarly, if there is a shift towards lower temperatures, then the rate of weathering is decreased, and therefore the temperature equilibrium is achieved again by the output of volcanic degassing introducing CO_2 back into the atmosphere and thus enhancing the greenhouse effect (Foley, 2015). These temperature fluctuations to higher or lower values can occur from changes in solar luminosity over time, for example leading to global ice-ages or moist greenhouse states (Foley, 2015). By this regulatory mechanism, it is believed that climate stability can be maintained over periods of geologic time, important for the habitability of our planet and the evolution of life as we know it (Walker, Hays, and Kasting, 1981).

Another important quantity to consider for a planet with active plate tectonics is the mean plate speed. This directly affects the atmospheric CO_2 pressure from the rate of degassing since a mantle with a higher temperature has lower viscosity, resulting in a higher mantle convection rate, higher plate speed, more CO_2 degassing from arc volcanism and ultimately a higher atmospheric CO_2 pressure. This increases surface temperatures via the greenhouse effect, increasing the rate of silicate weathering and therefore also drawing more CO_2 from of the atmosphere over geologic timescales.

1.5 Aims & Outline

Due to the abundance of low-mass stars in the Milky Way, in particular M-dwarfs, the potential for discovering a habitable system with a rocky, terrestrial planet is considered relatively high. With the longer evolutionary timescales of main sequence lifetimes in the billions and even trillions of years, it is believed that these stars could be suitable to host life for long periods of time, longer than for the Earth-Sun system. In this thesis, the evolution of surface conditions for Earth-like exoplanets orbiting M-K stars (stellar masses $0.1 - 1\,M_\odot$) will be considered through a numerical model of the carbon cycle and planetary evolution. We will consider timescales up to 20 Gyr, due to the longer main sequence lifetimes of these types of low-mass stars.

In this work, we focus on the atmospheric carbon dioxide pressure P_{CO_2} and surface temperature T_{surf} for their relevance in the carbon cycle model acting as a climate regulating mechanism over geological timescales via the greenhouse effect. The effects of the changing climate will be linked to the interior planetary evolution via the mean plate speed or the stellar luminosity evolution as an exterior process. In section 2, the carbon cycle model and its application is described. Here, the Earth-Sun model is presented for comparison to later

results in terms of habitability conditions. The last subsection of this chapter mentions how the original model is adapted to allow the study of lower mass stars than the Sun. Section 3 presents the methods and processes to obtain the results, beginning with an overview of how the luminosity evolution is calculated. Section 4 presents the results, beginning with an exoplanet around a $0.1\,\mathrm{M}_\odot$ and $0.5\,\mathrm{M}_\odot$ star receiving the same stellar irradiance on the surface as the Earth does from the Sun at $t = 0$. This is to determine the when stellar evolution begins to play a dominating role in affecting the surface conditions of T_{surf} and $P_{\mathrm{CO_2}}$ over interior planetary processes. Subsequently, a range of five different circumstellar distances are selected, from which habitable zone limits can be determined. Lastly, a model of Proxima Centauri b is performed, where a higher mass planet than the Earth is considered and the effects this has on the long-term habitability. Following this, a discussion is provided in section 5 where several considerations omitted in this work are described for possible future research. Finally, the conclusions are presented in section 6.

2 Carbon Cycle Model

In this thesis, we use a numerical box model, adapted from the work of Oosterloo (2020), to calculate the surface temperature T_{surf} and atmospheric CO_2 pressure P_{CO_2} of an Earth-like exoplanet around a low-mass star. As discussed previously, the carbon cycle is a necessary negative feedback mechanism which is able to maintain habitable surface conditions on the Earth. By applying this model to different Earth-like exoplanets, we aim to determine if they are habitable for long periods of time. We consider the initial stages of the main sequence evolution of such stars up to 20 Gyr. The pre-main sequence phase is excluded taking into account planet formation timescales and the variable stellar luminosity during this period, as well as the prevalence of strong stellar flares in the first 1 Gyr of M-dwarf lifetimes. Due to the extensive main sequence lifetimes of these low-mass stars, the post-main sequence phases are not considered. The original model can be applied to study Earth-like exoplanets orbiting a solar-type star, which we extend in this thesis to include stars of lower mass.

2.1 Model Description

The model considers the evolution of the Earth from its fully-formed state, with a convective mantle and active plate tectonics. The mean plate speed in the model for the Earth-like planet is only a function of T_{surf}, in turn determined by the P_{CO_2} (Oosterloo, 2020). This carbon cycle model only consists of the inorganic component, otherwise known as the long-term carbon cycle, which is the dominant climate regulator based on P_{CO_2} on Earth (Oosterloo, 2020). Therefore, the effects of the biosphere are disregarded. The model variables are four reservoirs, each indicating the amount of carbon (in moles) present in the atmosphere R_a, ocean R_o, crust R_c and the mantle R_m reservoirs (Oosterloo, 2020). The atmosphere and ocean reservoirs are coupled together into the surface reservoir $R_o + R_a = R_s$, as instantaneous equilibrium between R_a and R_o is assumed (Foley, 2015). The oceanic crust reservoir also includes the carbon from continental weathering in the continental crust, not individually modeled since it has a negligible influence on the feedback mechanisms (Oosterloo, 2020). The total carbon content, calculated as the sum of these reservoirs, is given by R_{tot} with a constant value of 2.5×10^{22} moles (Oosterloo, 2020). We only consider the initial condition ($t = 0$) of the carbon content fully in the surface reservoir ($R_s = 1$), and none in the crust and mantle reservoirs. However, different initial distributions of carbon converge after 1 Gyr and so it is not significant for the long-term evolution of the model (Oosterloo, 2020). The time derivatives of the reservoirs are calculated, from which we observe the changing amounts of carbon in each reservoir after a specific point in time.

The mass conservation equations below are the key equations for this model:

$$\frac{d(R_a + R_o)}{dt} = F_{\text{ridge}} + F_{\text{arc}} - \frac{F_{\text{weather}}}{2} - F_{\text{sfw}}. \tag{2}$$

$$\frac{dR_c}{dt} = \frac{F_{\text{weather}}}{2} + F_{\text{sfw}} - F_{\text{sub}}. \tag{3}$$

$$\frac{dR_m}{dt} = (1 - f)F_{\text{sub}} - F_{\text{ridge}}. \tag{4}$$

Here, F_{ridge} is the carbon flux (in units of moles per unit time) due to mid-oceanic ridge degassing of carbon from the mantle, f is the fraction of carbon degassed during subduction, with a fixed value of 0.5 (Foley, 2015), $F_{\text{arc}} = fF_{\text{sub}}$ represents arc volcanism degassing of CO_2 from subduction zones, F_{sub} is the subduction zone carbon flux, F_{weather} represents the effect of continental weathering and consequent extraction of CO_2 from the atmosphere. This value is linearly dependent upon the partial atmospheric CO_2 pressure, but exponentially dependent on the surface temperature, and thus a small change in the surface temperature will induce a large difference in the weathering flux (Oosterloo, 2020). Finally, F_{sfw} represents the seafloor weathering carbon flux. Equations $2 - 4$ are integrated over time to obtain the evolution of the four reservoirs R_a, R_o, R_c and R_m. Throughout the model, all fluxes are linearly dependent on mean plate speed except the rate of continental weathering. For the full parameterization of the fluxes and full model overview, see Oosterloo (2020).

To calculate the partial atmospheric CO_2 pressure (P_{CO_2}) considering CO_2 as an ideal gas, the following relation is used, known as Henry's law (Oosterloo, 2020; Foley, 2015):

$$P_{CO_2} = k_c x_c = k_c \frac{R_o}{M_{H_2O} + R_o}. \tag{5}$$

Here, k_c denotes CO_2 solubility in seawater (10^7 Pa) and x_c the mole fraction of CO_2 contained in the ocean and obtained from R_o, i.e. the amount of dilute CO_2 and the amount of water M_{H_2O} (7.6×10^{22} mol) in the oceans. Another way to represent P_{CO_2} is via the reservoir of carbon in the atmosphere, R_a, with the following relation (Oosterloo, 2020):

$$P_{CO_2} = \frac{R_a m_{CO_2} g}{A_m}. \tag{6}$$

Here, m_{CO_2} is the molar mass of carbon dioxide ($44\,\text{g}\,\text{mol}^{-1}$), g is the surface gravity ($9.8\,\text{m}\,\text{s}^{-2}$) and A_m ($5.1 \times 10^{14}\,\text{m}^2$) the surface area of the Earth (corresponding to the surface area of the mantle in this model).

The other quantity to be studied, the surface temperature of the planet T_{surf}, is determined as follows. The overall surface temperature is given as (Oosterloo, 2020; Walker, Hays, and Kasting, 1981):

$$T_{\text{surf}} = T_{s,\oplus} + 2(T_e - T_{e,\oplus}) + 4.6\left[\left(\frac{P_{\text{CO}_2}}{P_{\text{CO}_{2,\oplus}}}\right)^{0.346} - 1\right]. \tag{7}$$

Here $T_{s,\oplus}$ is the Earth's current average surface temperature of 285 K. T_e is the planetary effective temperature, with $T_{e,\oplus}$ the current value of effective temperature for the Earth (254 K) and $P_{\text{CO}_{2,\oplus}}$ is the present day partial CO_2 pressure on Earth (33 Pa), these values are obtained from Oosterloo (2020). The effective temperature is calculated by:

$$T_e = \left(\frac{S_{\text{irr}}(1-A)}{4\sigma}\right)^{1/4}. \tag{8}$$

Here, S_{irr} is the value for the stellar irradiance, A is the average albedo of the Earth (fixed at the present-day value of 0.31), and σ is the Stefan-Boltzmann constant. Since the solar irradiance evolves over time with solar evolution, the flux received on Earth during the course of the Sun's main sequence lifetime can be described by the following the relation, given by Gough (1981):

$$S_{\text{irr}}(t) = \frac{S_\odot}{1 + \frac{2}{5}(1 - t/t_\odot)}. \tag{9}$$

Here, $t_\odot$ is taken to be the current age of the Sun (4.5 Gyr) and $S_\odot$ is the solar constant $\sim 1360\,\text{W m}^{-2}$ (present solar irradiance on Earth).

For our model, we consider two cases, namely the coupled (allowing the plate speed to vary as a function of mantle temperature) and the uncoupled (fixing the plate speed at the present-day Earth value) scenarios. The coupled relation takes into account the cooling of the mantle, and thus its convective properties in connection to the mean plate speed over time. This influences the surface temperature and the atmospheric CO_2 pressure via the carbon cycle over tens of millions of years (Oosterloo, 2020).

2.2 Model for the Earth - Sun System

It is important to apply the model to the Earth and Sun system to obtain a baseline for habitability and to determine how a solar-type star evolving over its main sequence lifetime affects planetary surface conditions, before extrapolating this to a star of lower mass. Here, we model the evolution of T_{surf} and P_{CO_2} for the Earth. The results are shown in Figure 2 (a)

and (b), respectively. Both models for the coupled (continuous black curve) and uncoupled (dashed black curve) scenarios are shown to see the effects of the thermal evolution of the mantle on surface conditions. In Figure 2a, the boiling and freezing points of water are indicated with the red (373 K) and light-blue (273 K) dashed lines respectively, with the upper limit of 343 K as a habitability condition indicated by the green dashed line. In this study we consider surface temperatures of $273 - 343$ K to be the upper and lower habitable limits, between the ice-house effect beyond 248 K and the runaway greenhouse effect above 355 K (Lehmer, Catling, and Krissansen-Totton, 2020). The red dashed line in Figure 2b represents the minimum P_{CO_2} hospitable to life, with a value of 0.101 Pa (for a standard atmospheric pressure of 101.325 kPa) or 1 ppm CO_2. The blue dot in all subsequent figures represents the present-day value for the Earth (at 4.5 Gyr).

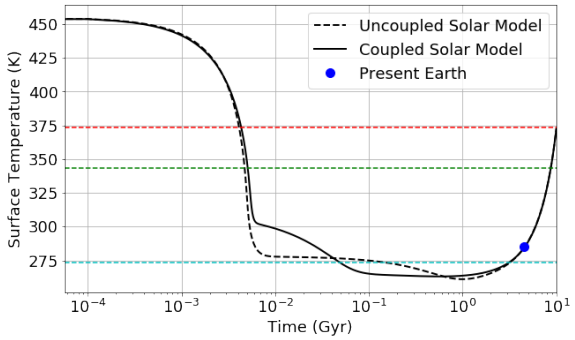

(a) Surface temperature T_{surf} (K). Blue dot indicates present-Earth average value of 285 K.

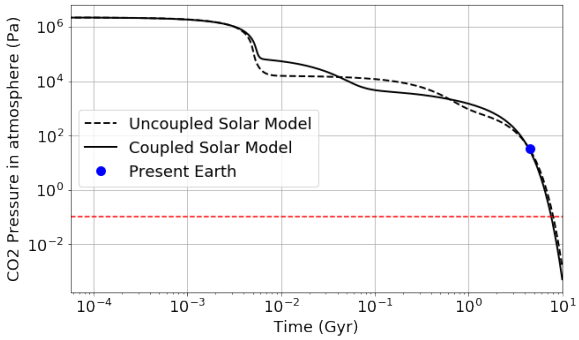

(b) Atmospheric CO_2 pressure P_{CO_2} (Pa). Blue dot indicates present-day average Earth value of 33 Pa.

Figure 2: Long-term evolution for the Earth model. Red dashed line in (a) represents the boiling point of water (373 K), the light-blue line the freezing point (273 K) and the green line the maximum habitable temperature (343 K). The red dashed line in (b) shows minimum habitable CO_2 pressure of 0.101 Pa.

Even though the surface temperature in Figure 2a is very high at $t = 0$, with a value of approximately 450 K, after $\sim 5 \times 10^{-3}$ Gyr a more stable scenario is reached and maintained for several millions of years. These initially high surface temperatures are due to the distribution of carbon fully in the atmosphere reservoir, with the rate of CO_2 able to be extracted from the atmosphere determined by the 'supply-limited' weathering regime. This prevents the weathering rate from increasing exponentially as a function of T_{surf} and P_{CO_2} (Oosterloo, 2020). The initial value of P_{CO_2} at $\sim 10^6$ Pa in Figure 2b is again determined by the reservoir distribution of carbon in the atmosphere. Up to $\sim 0.1 - 1$ Gyr, the various reservoirs are still in the process of reaching their equilibrium values (Oosterloo, 2020). Afterwards, a small difference in P_{CO_2} arises between the coupled and the uncoupled model. The coupled model predicts more CO_2 in the atmosphere between approximately $1 - 4.5$ Gyr than the uncoupled model due to the fact that a hotter mantle results in a higher plate speed in this model. Hence, more degassing occurs at earlier times than on the present-day Earth. However, the evolution of the Sun plays an important role, most prominently after 4.5 Gyr, after this initial

adjustment period. Here, the increasing solar luminosity starts to dominate the evolution of atmospheric CO_2, due to increased surface temperatures and hence the two models react similarly to exterior changes in stellar luminosity. As the Sun begins exhausting its hydrogen reserves in its core, there are fewer fusion reactions taking place per cubic cm, but the inward pressure remains the same, speeding up the process of fusion of the remaining hydrogen and thus causing the increase in solar luminosity (Christensen-Dalsgaard, 2021). This increases the surface temperature of the Earth, subsequently increasing the silicate weathering rate, drawing more CO_2 out of the atmosphere and acting to balance the temperature in a period of geologic time.

With increasing surface temperatures (directly related to the solar luminosity and hence increased flux on the Earth), continental weathering rates for the uncoupled model are enhanced and thus more CO_2 is extracted from the atmosphere and drawn down into the mantle, while the rate of degassing remains the same (Rushby et al., 2018). This explains the decreasing trend in Figure 2b and the higher rate of CO_2 extraction from the atmosphere as the Sun significantly increases in luminosity. For the coupled scenario, the degassing rate is decreasing over time due to the cooling of the mantle and thus a decreased plate speed leads to reduced volcanism activity, meaning less CO_2 released into the atmosphere. These two quantities of the planetary surface temperature and atmospheric CO_2 pressure will therefore serve as the standard metric to help determine if Earth-like exoplanets around stars of mass lower than the Sun can be habitable for long periods of time.

With an understanding of how interior (planetary) and exterior (stellar) processes affect surface conditions T_{surf} and P_{CO_2} on an Earth-like planet over long periods of time, we can apply the model to stars of lower mass than the Sun.

3 Methodology

Since low-mass stars are present in such high abundance throughout our galaxy, it is important to consider them as likely candidates for the possible existence of extraterrestrial lifeforms on their orbiting exoplanets. In order to determine whether life can survive and evolve for sufficiently long timescales, the long-term evolution of these types of stars must be considered. The original model from Oosterloo (2020) can only take into account the main sequence evolution for the Sun, therefore it had to be adapted to take into account stars of lower mass and their corresponding evolutionary timescales with significantly longer main sequence lifetimes. The stellar luminosity evolution will then be used in the carbon cycle model to see how the surface conditions (T_{surf} and P_{CO_2}) of the Earth-like exoplanet are affected over long periods of time to determine potential habitability.

3.1 Stellar Luminosity Evolution

The evolution of luminosity of various types of stars (based on their mass) is determined from the existing stellar evolution code of Siess, Dufour, and Forestini (2000). Here, a solar metallicity, Z = 0.020, X = 0.703, Y = 0.277, was assumed, where X, Y and Z are, respectively, the mass fractions of hydrogen, helium, and heavy elements. The stellar evolution tables contain information for different stellar masses in the range $0.1 - 1\,\mathrm{M}_{\odot}$, and we extracted the luminosity and corresponding time, shown below in Figure 3. Note that both the pre-main sequence and main sequence phases are shown.

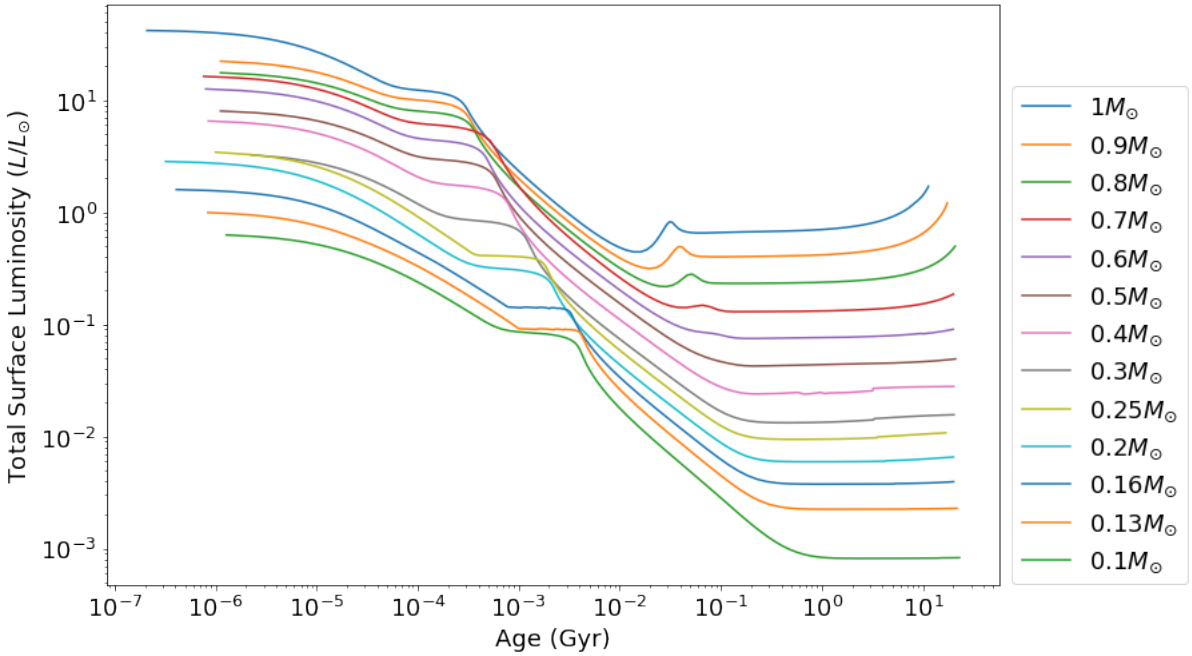

Figure 3: Stellar luminosity (in solar units) evolutionary tracks (pre-main sequence and main sequence) for $0.1\,\mathrm{M}_{\odot} \leqslant \mathrm{M} \leqslant 1\,\mathrm{M}_{\odot}$ with data from Siess, Dufour, and Forestini (2000).

Since the stellar evolutionary tables from Siess, Dufour, and Forestini (2000) provide the luminosity of the star, it is necessary to convert this into stellar irradiance to determine the flux on the surface of the exoplanet. The stellar irradiance S_{irr}, measured in $\mathrm{W\,m^{-2}}$, received on a planet for any star can be calculated from the stellar luminosity L (in solar units) at a particular circumstellar distance d (in metres) by the following relation, adapted from LeBlanc (2011):

$$S_{\mathrm{irr}}(t) = \frac{L(t)}{4\pi d^2}. \tag{10}$$

It was necessary to convert the solar irradiance in the original model of Oosterloo (2020) using eq. (10) and divide this by the value of the present solar luminosity to get the value in $L_{\odot}$. With the stellar evolutionary track for a $1\,\mathrm{M}_{\odot}$ star from Siess, Dufour, and Forestini (2000) and the standard solar evolution model from Oosterloo (2020), we can compare the two models for the main sequence. The red dashed line in Figure 4 represents the model from Oosterloo (2020) used for the varying solar luminosity with time (eq. (9)). This relation is only valid for the main sequence lifetime of the Sun, and thus the track starts at 0.05 Gyr and ends at 10 Gyr (Oosterloo, 2020). To calculate the residual between the luminosity of the standard solar model (SSM) of Oosterloo (2020) and the stellar evolutionary track (SET) of Siess, Dufour, and Forestini (2000) for a $1\,\mathrm{M}_{\odot}$ star from (Siess, Dufour, and Forestini, 2000), the following formula was used:

$$\%\ \text{residual} = \frac{\text{SSM - SET}}{\text{SET}} \times 100\ \%. \tag{11}$$

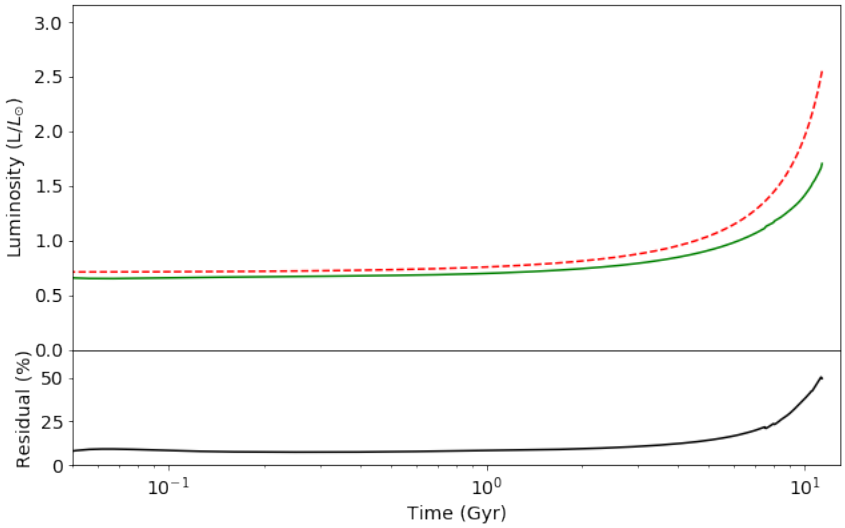

Figure 4: Residual (percentage) plot for Oosterloo (2020) solar evolution model (red dashed line) and data for a $1\,\mathrm{M}_{\odot}$ star from Siess, Dufour, and Forestini (2000) (green smooth curve).

From Figure 4, the two models can be seen to have $\sim 10\%$ deviation for the first 1 Gyr, after which the residual increases more significantly to $\sim 50\%$ at 10 Gyr. The two models are relatively similarly up to ~ 3 Gyr, after which a systematic deviation increases the difference between the two models. The standard solar model of (Oosterloo, 2020) will be used to compare the results for different stellar masses to stay comparable to his work.

With this approach, we are able to calculate the necessary quantities from the carbon cycle model, such as the atmospheric CO_2 pressure and the surface temperature of the Earth-like exoplanet around the low-mass star with significantly different stellar evolution in comparison to a solar type star.

3.2 Stellar Luminosity Interpolation & Extrapolation

To find a similar relation as the solar luminosity evolution for low-mass stars, an interpolation routine was carried out for the stellar luminosity evolution over time from the data curves of Siess, Dufour, and Forestini (2000) in Figure 3. We performed a 1D linear interpolation routine between time and mass for all of the stellar masses for which data was available between $0.1 - 1\,M_\odot$ from Siess, Dufour, and Forestini (2000) between a time range of $10^{-5} - 10$ Gyr, interpolated on a logarithmic time grid the same for all stars. This is necessary to ensure that the data is all taken on the same time range to be able to compare models for different stellar masses later on. The results of this are shown in Figure 5 where the black lines represent the 1D interpolated values above the model data points.

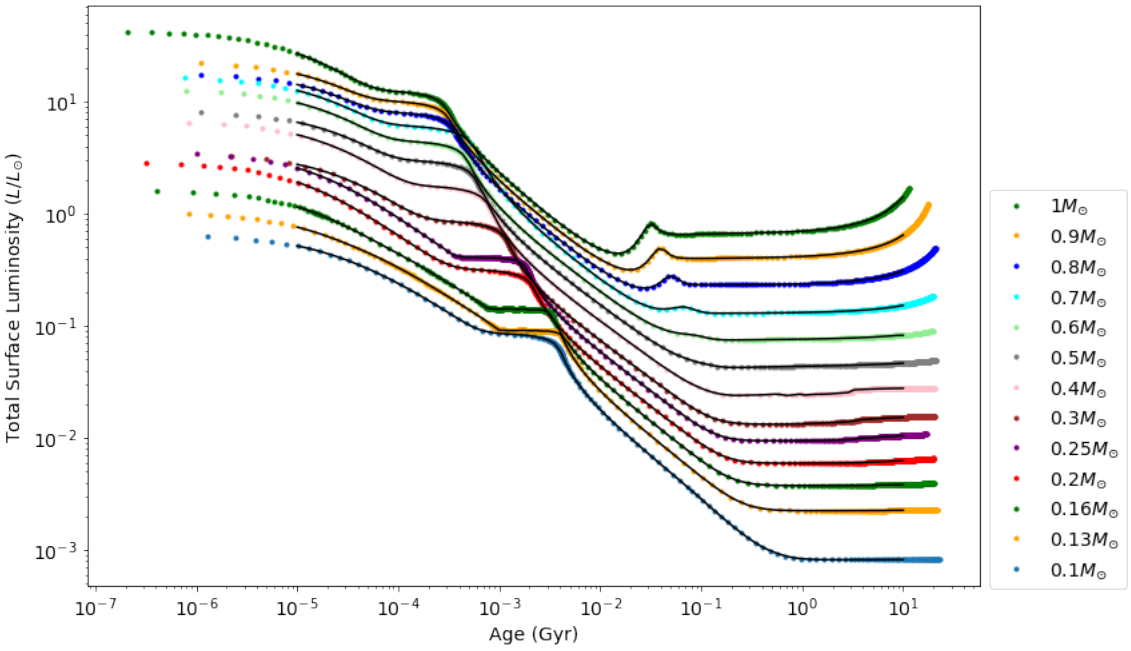

Figure 5: 1D interpolation routine for $0.1 - 1\,M_\odot$ stars up from 10^{-5} to 10 Gyr and model data points from (Siess, Dufour, and Forestini, 2000).

Now that we have the stellar luminosity evolutionary tracks for various masses, we can use a second interpolation routine to find the luminosity evolution for any stellar mass within this range. A 2D interpolation routine was carried out in order to determine the luminosity as a function of stellar age and mass. For the first trial, the interpolation routine was taken up to 10 Gyr, since all evolutionary tracks are available up to this value. These results will later be extended to 20 Gyr as the main sequence lifetimes of these low-mass stars extend far beyond the end of the main sequence of the Sun.

The 2D linear interpolation for the luminosity as a function of stellar mass and age is shown below in Figure 6. The white contour lines indicate where the luminosity is constant, showing the general trend of higher or lower luminosity. The dashed lines indicate values for the luminosity L lower than $L_\odot$, and smooth lines indicating values above $L_\odot$. The figure should be read horizontally from left to right following the luminosity evolution for a particular stellar mass over time.

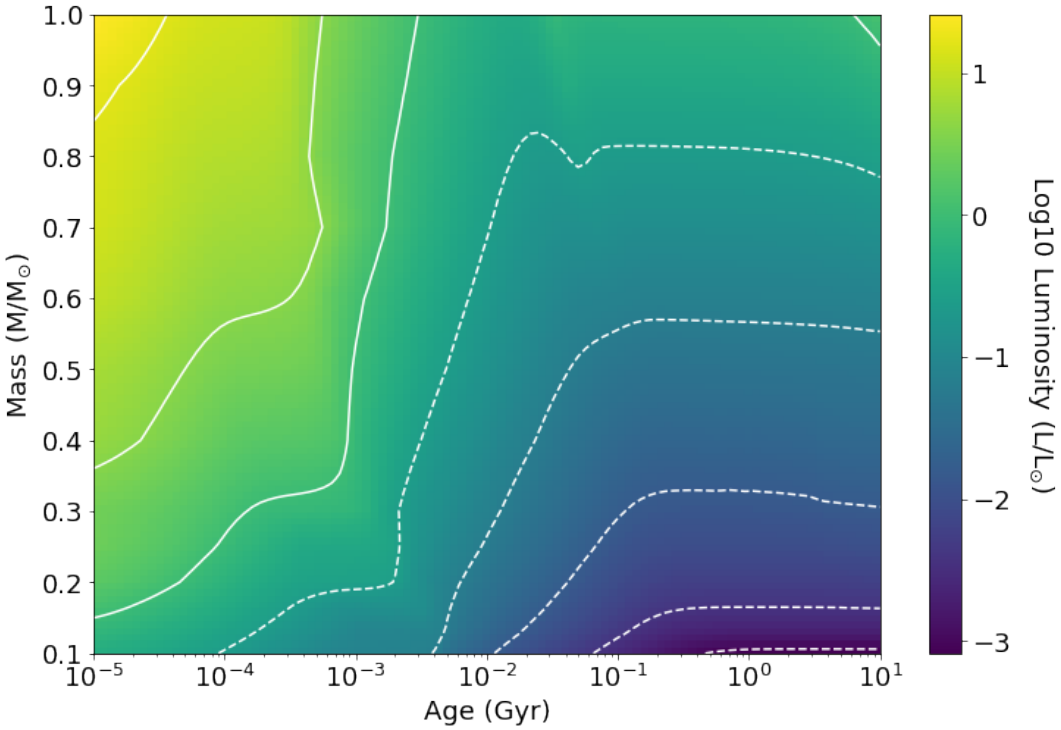

Figure 6: 2D interpolated color and contour plot of how the stellar luminosity (in solar units) changes with mass over time (log-scale) for the range $0.1 - 1\,M_\odot$.

In order to extend this model up to 20 Gyr, a similar interpolation routine was carried out as previously described, except that now the stellar masses above $0.7\,M_\odot$ have been omitted since their main sequence lifetimes end before 20 Gyr. There are only two stellar masses from the evolutionary tracks of Siess, Dufour, and Forestini (2000) that do not cover the full evolution up to or beyond 20 Gyr, namely for $0.25\,M_\odot$ and $0.6\,M_\odot$, which go up to ~ 17 Gyr and just below 20 Gyr respectively. It is considered reasonable therefore to extrapolate for

the stellar masses and include the values up to 20 Gyr for the rest of the model data available. A linear extrapolation routine was performed for these two stellar masses, after which the same 2D interpolation routine as in the previous case was carried out.

The deviation between the 2D interpolated values (of luminosity evolution with time for all stellar masses) and the model data from Siess, Dufour, and Forestini (2000) is performed, the results of which are shown below in Figure 7 and Figure 8 for a $0.1\,M_\odot$ and $0.5\,M_\odot$ mass star, respectively. These two masses are selected to take into account the lowest-mass star and an intermediate mass star from the model with different main sequence lifetimes. A similar version as eq. (11), now with the interpolated data instead of SSM, was used to calculate the residuals, given as a percentage. Residual plots for all stellar masses for which the evolutionary tracks were available from (Siess, Dufour, and Forestini, 2000) have been calculated, but are omitted for simplicity.

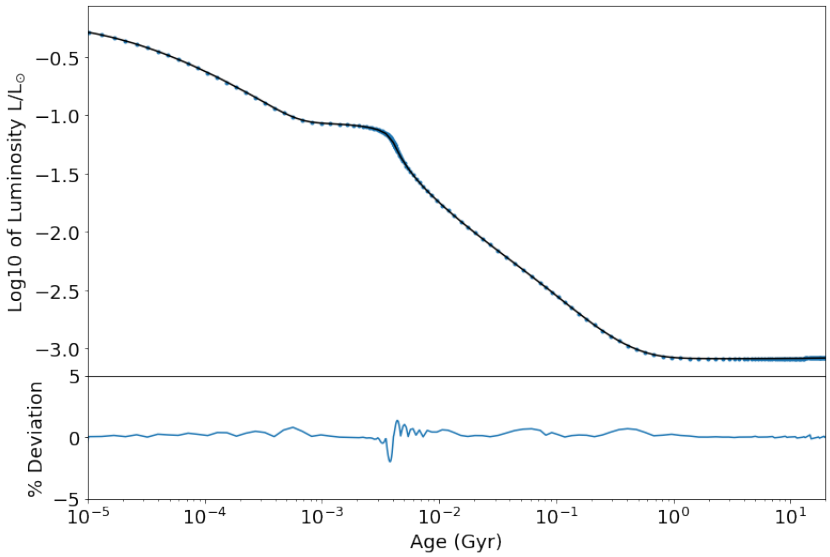

Figure 7: 20 Gyr evolution for 2D interpolated values (black line) with the data from Siess, Dufour, and Forestini (2000) for $0.1\,M_\odot$ (blue points) and percentage deviation in lower plot over a logarithmic time axis.

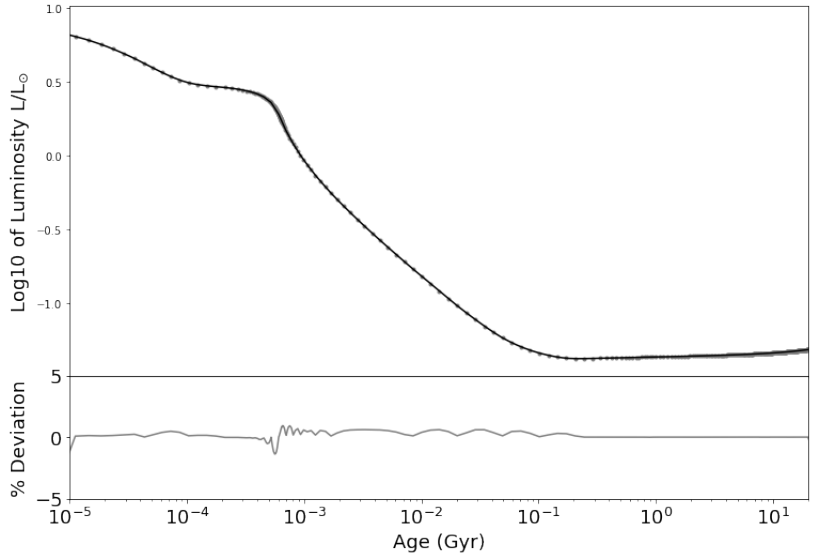

Figure 8: 20 Gyr evolution for 2D interpolated values (black line) with the data from Siess, Dufour, and Forestini (2000) for $0.5\,M_\odot$ (grey points) and percentage deviation in lower plot over a logarithmic time axis.

None of the residuals in Figure 7 and Figure 8 or the rest of the stellar evolutionary tracks between the interpolated values and model data points surpass 4%, indicating that the interpolation routine accurately represents the model data between the selected time range. It is not expected that such a small deviation will cause errors or over- or under-estimations in the calculations of T_{surf} and P_{CO_2}. Now, the stellar evolutionary tracks can be inserted into the carbon cycle model to calculate the necessary quantities of T_{surf} and P_{CO_2} to determine the possible long-term habitability of Earth-like exoplanets around these low-mass stars.

4 Results

In order to assess the possible long-term habitability of Earth-like exoplanets around low-mass stars, the model of the carbon cycle and planetary evolution is applied to these systems to determine the surface temperature T_{surf} and atmospheric CO_2 pressure P_{CO_2} over time. These are deemed to be the most important quantities for habitability, relevant for the greenhouse effect and the carbon cycle acting as a climate regulating mechanism. By exploring various distances of the exoplanet to the central star, the optimal region can be determined for possible long-term habitability based on a range of temperatures to sustain surface liquid water over geologic timescales. This is a prerequisite for the existence and survival of known carbon-based life. The effect of stellar evolution will be studied to see how it affects surface conditions along with interior planetary processes in comparison to the Earth.

In section 4.1 we model an Earth-like exoplanet orbiting at a distance where it receives the same stellar irradiation as the Earth at the initial time $t = 0$. This is to differentiate between the effects of planetary evolution from those of stellar evolution especially at longer timescales up to 20 Gyr. Subsequently, the distance to the star is changed to determine a range of possible habitable distances based on T_{surf} and P_{CO_2} between the habitable range of $273 - 343$ K and above 0.101 Pa, respectively. We calculate both cases for the uncoupled and coupled models (described in section 2.1). With the uncoupled case, only the evolution of the stellar luminosity over time and its direct effects on the surface conditions of the planet are considered, without the effects of internal planetary evolution. This is compared to the coupled model, where the carbon cycle is coupled to the thermal evolution of the mantle via the plate speed, and thus internal physical processes can play a larger role in determining the surface conditions of the planet (Oosterloo, 2020). In section 4.3, we apply the model to the system of Proxima Centauri b, to draw relevant conclusions on the long-term evolution of the planet's surface conditions and consequences for habitability.

4.1 Earth analogs around low-mass stars

Since we are interested in low-mass stars of M-K spectral type for their abundance in our galaxy, we present the results for a $0.1\,M_\odot$ and $0.5\,M_\odot$ mass star with an orbiting Earth-like exoplanet. The luminosity for the lower mass star is $\sim 1\%$ that of the Sun. Since this is the lowest mass star considered, it also has the longest main sequence lifetime of ~ 3160 Gyr, calculated from eq. (1). Meanwhile, the $0.5\,M_\odot$ star has a slightly higher luminosity of $\sim 4\%$ that of the Sun. The luminosity of stars of mass $M \lesssim 0.5\,M_\odot$ will not change significantly during the course of their main sequence lifetimes as hydrogen fusion proceeds at very slow rates (due to their small size and being mostly convective) (LeBlanc, 2011). Due to these faint luminosities, the habitable region must lie very close to the star, much closer than the Earth-Sun distance, in order to receive enough stellar irradiation to keep the planet within a habitable temperature range to sustain liquid water. An offset of 1 Gyr is selected between the beginning of stellar evolution and the beginning of the carbon cycle model. This allows sufficient time for the full formation of the Earth-like planet, as well as for the low-mass stars

to evolve onto the initial stages of their main sequence lifetimes. Thus, a relatively stable luminosity is maintained for several billions of years, which can be a positive consideration for the long-term habitability of their exoplanets. Additionally, since M-dwarfs are renowned for their violent stellar flares, most active in the first 1 Gyr of their lifetimes, this can be avoided with such an offset.

Firstly, we show the stellar irradiation received on the exoplanets of stars of mass $0.1\,M_\odot$ and $0.5\,M_\odot$, with the exoplanet placed at distances 0.0342 AU and 0.247 AU, respectively. These distances are chosen such that the stellar radiation received at $t = 0$ is the same as the Earth, as shown below in Figure 9 with the orange and blue curves representing the stellar irradiance received on the surface of an Earth-like exoplanet around a star of mass $0.1\,M_\odot$ and $0.5\,M_\odot$, respectively. The present-day value of $S_{\rm irr} = 1360\,{\rm W\,m^{-2}}$ on Earth is indicated by the blue dot.

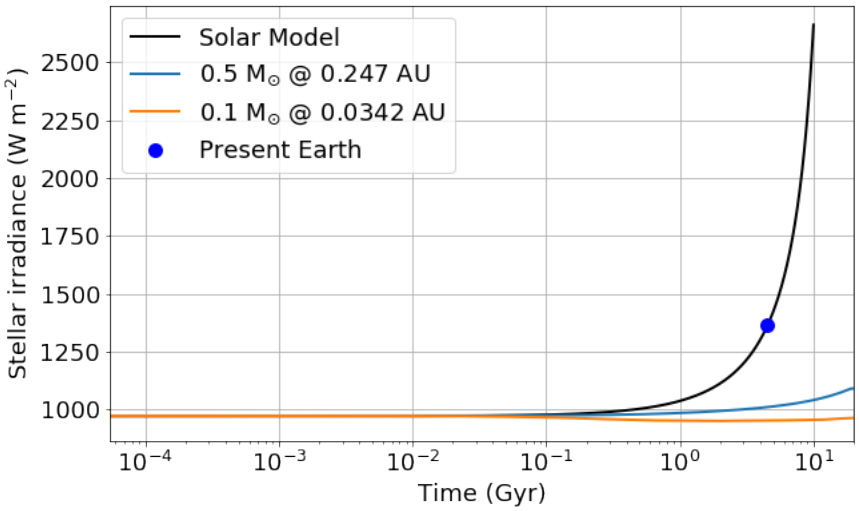

Figure 9: Stellar irradiance ($\rm W\,m^{-2}$) evolution received on the Earth from the Sun (black line) with the blue dot indicating the present-day value of $\sim 1360\,\rm W\,m^{-2}$, an Earth-like exoplanet of a $0.1\,M_\odot$ mass star at $d = 0.0342$ AU (orange line) and an Earth-like exoplanet of a $0.5\,M_\odot$ mass star at $d = 0.247$ AU (blue line) to receive the same value as the Earth at $t = 0$.

Here the different stellar evolution for the three different mass stars can be seen from $\sim$ 0.1 Gyr, with large deviation in irradiance thereafter. The first results in Figure 10 (a) and (b) show the surface temperature $T_{\rm surf}$ and atmospheric CO_2 pressure P_{CO_2} evolution, respectively, for an Earth-like exoplanet of a $0.1\,M_\odot$ or $0.5\,M_\odot$ mass star. The uncoupled (black dashed curve) and coupled cases (black continuous curve) for the Earth-Sun model are also shown for comparison. The present-day Earth values are also indicated by the blue dots of $T_{\rm surf} = 285\,\rm K$ and $P_{CO_2} = 33\,\rm Pa$.

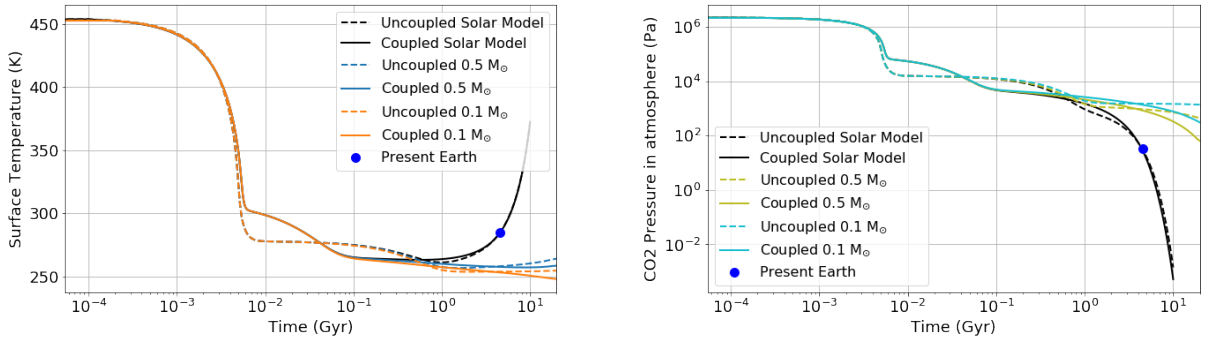

(a) Surface temperature T_{surf} (K). Blue dot indicates present-Earth value of 285 K.

(b) Atmospheric CO_2 pressure P_{CO_2} (Pa). Blue dot indicates present-day Earth value of 33 Pa.

Figure 10: Evolution of surface conditions on Earth-like exoplanet around a 0.1 $M_\odot$ star at a distance of 0.0342 AU and 0.5 $M_\odot$ star at a distance of 0.247 AU. The black curves represent the Earth-Sun model with the blue dots indicating the present-day values.

In Figure 10, T_{surf} and P_{CO_2} on both the Earth and the Earth-like exoplanets for both the uncoupled and coupled models initially have the same value ($T_{\text{surf}} \sim 450$ K and $P_{CO_2} \sim 10^6$ Pa) since all three planet systems receive the same stellar irradiance. The initial phase from up to $\sim 10^{-3}$ Gyr can be attributed to the surface temperature dependence on the supply-limited regime of the carbon cycle model. Therefore, initially, the T_{surf} and P_{CO_2} dependence is only on interior (planetary) processes, and not the stellar evolution, since all three stellar systems (for the Sun, 0.1 $M_\odot$ and 0.5 $M_\odot$ stars) are still on the main sequence with relatively constant luminosity. Even with initially very high surface temperatures, surface water could still be maintained due to the high atmospheric CO_2 pressure, both for the Earth model and for the Earth-like exoplanets (Oosterloo, 2020). Once the supply-limited regime is surpassed, both the T_{surf} and P_{CO_2} significantly decrease as large amounts of carbon have been sequestered from the atmosphere, enough to induce a significant decrease in the surface temperature of ~ 150 K for the coupled model and ~ 175 K for the uncoupled model. At 5×10^{-3} Gyr, a large deviation between the coupled and uncoupled cases can be seen, which is attributed to the respective internal planetary process of mantle cooling. For the coupled models, the temperature decline stops at a slightly higher value with respect to the uncoupled models at ~ 300 K instead of ~ 275 K at 5×10^{-3} Gyr. This is due to the thermal evolution of the mantle, which slows down the surface cooling process initially, but then can be seen to bring the temperatures at approximately the same level with the coupled case at 5×10^{-1} Gyr for both stellar models.

In order to better visualize the long-term evolution, we show the same quantities of T_{surf} and P_{CO_2} on a linear time axis, obtaining the following results in Figure 11:

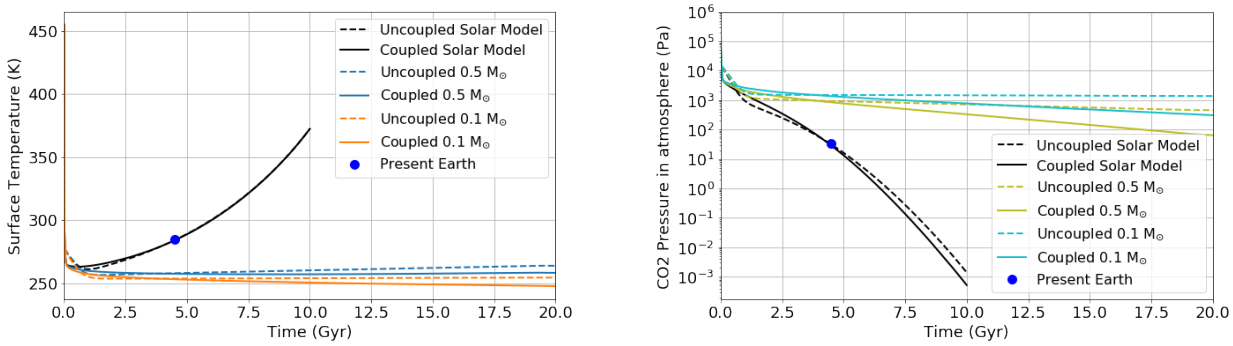

(a) Surface temperature (K). Blue dot indicates present-Earth value of 285 K.

(b) Atmospheric CO_2 pressure (Pa). Blue dot indicates present-day Earth value of 33 Pa.

Figure 11: Evolution of atmospheric CO_2 pressure for the Earth-Sun model and an Earth-like exoplanet around a 0.1 $M_\odot$ star at a distance of 0.0342 AU and a 0.5 $M_\odot$ star at a distance of 0.247 AU.

For a 0.1 $M_\odot$ star with the longest main sequence lifetime of a few thousand Gyr, its evolution is vastly different from that of the Sun, which already significantly increases in luminosity before it enters its red giant phase at 10 Gyr, as seen by the increasing T_{surf} in Figure 11a. The 0.5 $M_\odot$ star also have a relatively long main sequence lifetime of $\sim$ 56 Gyr, and its increasing luminosity can be seen to influence the surface conditions of T_{surf} and P_{CO_2} more than the lower mass star. The Sun's stellar evolution towards the end of its main sequence phase causes the Earth's surface temperature to increase rapidly at later stages, whilst the surface temperature on the Earth-like exoplanet around the lower-mass star stays more constant at slightly below the freezing point of water ($\sim$ 250 K for both coupled and uncoupled cases) by 20 Gyr. If the surface temperature drops below the freezing point of water for a few thousand years then the planet can freeze over, affecting the water-mediated carbon cycle to function as a climate regulating mechanism (Pierrehumbert, 2009). Thus, the planet will most likely experience the 'ice-house' effect, and remain indefinitely glaciated. For the atmospheric CO_2 pressure, there is a difference of several orders of magnitude, higher and relatively more stable, for the exoplanet than on Earth due to the slowly increasing stellar luminosity of the lower-mass star not affecting the silicate weathering rates as significantly. Meanwhile, the Earth which experiences an increase in surface temperatures due to the increasing luminosity of the Sun as it evolves, affecting T_{surf} and subsequently P_{CO_2} via the carbon cycle. However, even with high P_{CO_2} levels for the exoplanets, the temperatures remain very low for long timescales as the circumstellar distances are too far to receive sufficient stellar irradiation for a comfortably habitable climate.

Overall, for this case of an initial CO_2 distribution entirely in the surface (atmosphere and ocean) reservoir, i.e. with an initially very CO_2 rich atmosphere, the long-term evolution of the surface temperature and the atmospheric CO_2 pressure can be described as follows.

The first process that occurs where the stellar irradiance is the same, from 3×10^{-5} Gyr to $\sim 10^{-3}$ Gyr is supply-limited silicate weathering (Oosterloo, 2020). This is the process responsible for the removal of CO_2 from the atmosphere, requiring several millions of years before the P_{CO_2} decreases significantly and stabilizes the climate through the negative feedback mechanism of the carbon cycle. The high values of T_{surf} and P_{CO_2} remain relatively constant in the initial period up to $\sim 10^{-3}$ Gyr because of the supply-limited weathering regime. Only after $10^{-3} - 10^{-2}$ Gyr, an equilibrium is established between arc volcanism and weathering on the surface of the Earth and Earth-like exoplanet (Oosterloo, 2020). By 10^{-1} Gyr, the mantle reservoir has accumulated enough carbon to establish an equilibrium between ridge degassing and arc volcanism and weathering. During this stage, the quantity that plays an crucial role is the plate speed, due to its importance in the process of cycling the carbon extracted from the atmosphere into the mantle. After this point, the surface conditions of the planet are more affected by the stellar evolution, as seen by the increasing surface temperatures and decreasing atmospheric CO_2 pressure, than interior processes, which is the case until the end of the model at 20 Gyr.

The Earth will no longer be habitable when the Sun reaches its red-giant phase due to increased solar flux, but this problem is not encountered (at least not at this early stage) for these lower mass stars and their Earth-like exoplanets. The planets considered here, for the same stellar irradiation as the Earth at $t = 0$, experience far too cold temperatures to host life for long timescales. The next step is to see how the exoplanet distance to its central star affects T_{surf} and P_{CO_2} over time, up to 20 Gyr, and if habitable conditions can be sustained.

4.2 Exploring Various Circumstellar Distances

As was explored in the previous section, receiving the same stellar irradiance at $t = 0$ as the Earth does from the Sun does not mean that the exoplanet will be habitable for long periods of time. However, this allowed us to determine that stellar evolution begins to play a dominating role for T_{surf} and P_{CO_2} over interior planetary processes at a time of ~ 0.1 Gyr. It is not likely that an exoplanet will receive exactly the same stellar irradiation as on Earth, and thus altering the circumstellar distance allows us to determine the most optimal range for habitability on such an exoplanet around a low-mass star based on the T_{surf} and P_{CO_2} as a function of time.

We again apply the model to an Earth-like exoplanet, orbiting a star of mass $0.1\,M_\odot$ and $0.5\,M_\odot$. Here, five different distances are explored by taking into account the freezing point of water (273 K) and the upper habitable temperature limit of (343 K), indicated by the upper and lower black dashed lines in Figure 12a and Figure 13a, respectively. The lower habitable limit for the atmospheric CO_2 pressure is set to 0.101 Pa, indicated by the black dashed line in Figure 12b and Figure 13b. The two scenarios of the coupled and uncoupled planetary evolution models are shown, indicated by the continuous and dashed lines respectively. The blue dot in all figures indicates the present-day value for $T_{surf} = 285$ K and $P_{CO_2} = 33$ Pa for reference. The results presented below are taken on a linear time axis in order to better visualize the long-term effects.

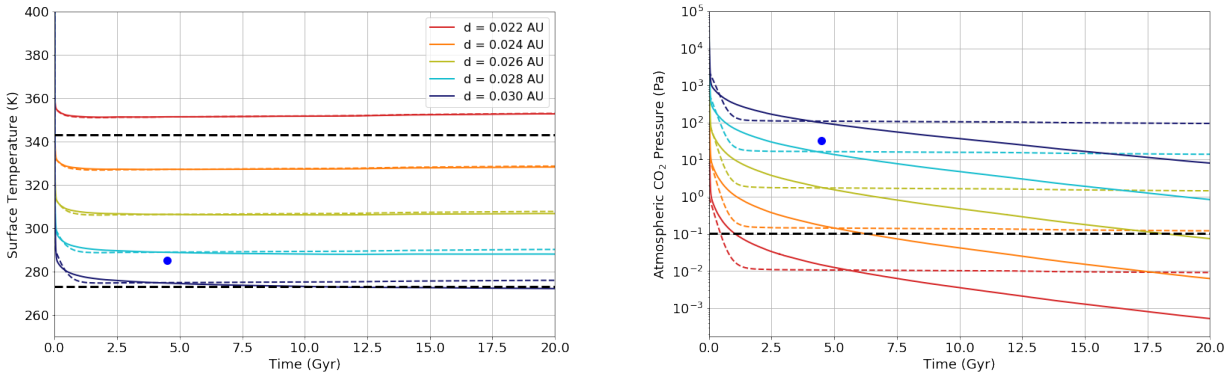

(a) Surface Temperature (K)

(b) Atmospheric CO_2 Pressure (Pa)

Figure 12: 20 Gyr evolution for a 0.1 $M_\odot$ star for an exoplanet at various distances. The blue dot represents the present-day Earth value of $T_{\text{surf}} = 285\,\text{K}$ and $P_{CO_2} = 33\,\text{Pa}$. Top and bottom black dashed lines in (a) represent the habitable conditions of 343 K and 273 K, respectively. Black dashed line in (b) represents minimum habitable condition of $P_{CO_2} = 0.101\,\text{Pa}$.

From the evolution of T_{surf} and P_{CO_2} up to 20 Gyr, shown in the two figures above, it can be said that the surface temperature on the exoplanet orbiting around a star of mass 0.1 $M_\odot$ experiences very constant temperatures from ~ 1 Gyr, with the outer- and inner-most boundaries plotted here considered uninhabitable. From Figure 12a, for the further distance of 0.03 AU, the surface temperature drops significantly in the first ~ 5 Gyr, experiencing sub-freezing temperatures beyond this point for the coupled case. This would most likely lead to a complete freezing of all surface water, and the 'ice-house' effect would ensue. By considering either the coupled or uncoupled case for this distance, the surface temperature could be above the minimum limit (as is the case if we do not consider the effects of mantle cooling) and thus considered habitable. For the planet closest in to the star, at a distance of 0.022 AU, the temperatures are always above the habitable limit of 343 K for the duration of the star's lifetime. At this temperature, the surface water would likely have evaporated by ~ 1 Gyr (Lehmer, Catling, and Krissansen-Totton, 2020). The other distances however, in the range $0.024 - 0.028$ AU are considered habitable for this portion of the star's main sequence lifetime, and probably until the end of its life, showing a very promising candidate for habitability at $d = 0.028$ AU considering the surface temperature of the present-day Earth ($T_{\text{surf}} = 285$ K).

In terms of P_{CO_2}, it can be seen that for a planet at 0.022 AU and for the coupled case of 0.024 AU, the CO_2 pressure eventually falls below the habitable limit of 0.101 Pa. This lower bound is almost immediately surpassed for the exoplanet at the closest distance of $d = 0.022$ AU, but for a planet at 0.024 AU this limit is surpassed at ~ 5 Gyr. Therefore, for these cases, the exoplanet would not be considered habitable for much longer periods of time than the Earth. The other CO_2 pressures for the other distances in the range 0.240 (uncoupled) – 0.028 AU are considered well-within the habitable range for several tens of billions of years.

For a $0.5\,M_\odot$ star, its main sequence lifetime is significantly shorter than the $0.1\,M_\odot$ star, and thus its luminosity evolution is likely to affect the planetary surface conditions of its orbiting Earth-like exoplanet to a larger extent. Figure 13a and Figure 13b show the long-term evolution of surface temperature and atmospheric CO_2 pressure, respectively. Here, the increase in stellar luminosity for a $0.5\,M_\odot$ star can be clearly seen affecting T_{surf} and P_{CO_2} more than for the lower mass star in the previous case. In terms of habitability up to 20 Gyr, the optimal distances for this particular stellar mass would lie in the range 0.180 AU to 0.220 AU, considering the freezing point of water and the habitable upper limit indicated by the bottom and top black dashed lines, respectively. Also considering P_{CO_2}, the most optimal scenarios would be for a distance of 0.20 AU to 0.180 AU (uncoupled), otherwise the lower limit of 0.101 Pa is surpassed relatively early, leading to uninhabitable conditions.

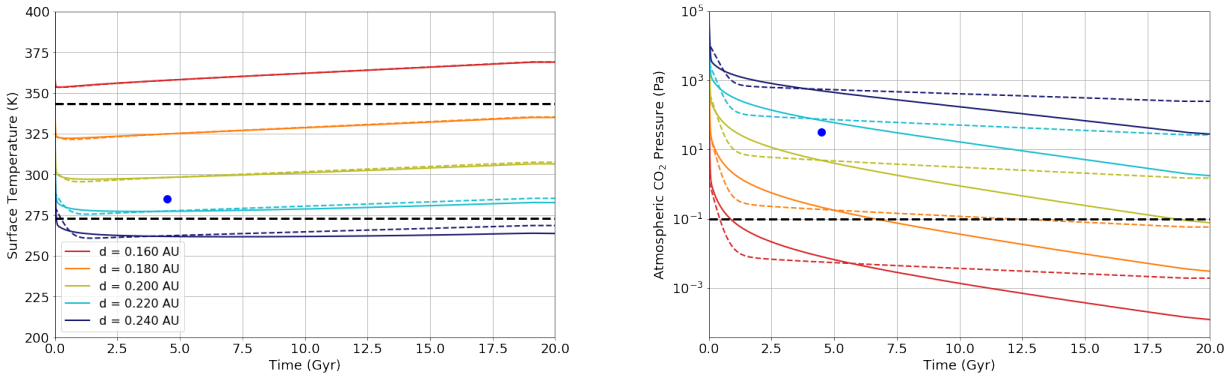

(a) Surface Temperature (K)

(b) Atmospheric CO_2 Pressure (Pa)

Figure 13: 20 Gyr evolution for a $0.5\,M_\odot$ star for an exoplanet at various distances. The blue dot represents the present-day Earth value of $T_{\text{surf}} = 285\,K$ and $P_{CO_2} = 33\,Pa$. Top and bottom black dashed lines in (a) represent the habitable conditions of 343 K and 273 K, respectively. Black dashed line in (b) represents minimum habitable condition of $P_{CO_2} = 0.101\,Pa$.

This $0.5\,M_\odot$ star has a wider range of habitable zone distances, extending from approximately 0.18 AU to 0.22 AU (range of 0.04 AU, based on the surface temperatures between $280 - 340\,K$). For the $0.1\,M_\odot$ star, the range of habitable distances is $\sim$ 0.023 AU to 0.029 AU (range of 0.006 AU). Therefore, for the higher mass system, a higher probability of finding a habitable planet for long periods of time exists since a wider range of distances can be considered habitable. However, the stellar evolution proceeds more quickly than for the $0.1\,M_\odot$ case, and so surface temperatures may become uninhabitable after several tens of billions of years on such an Earth-like exoplanet, also with the atmospheric CO_2 pressure most likely dropping below the habitable limit sooner than the T_{surf} limits are surpassed. All in all, these results indicate promising cases for the long-term habitability of Earth-like exoplanets around low-mass stars considering their surface conditions of T_{surf} and P_{CO_2} for up to 20 Gyr.

4.3 Applying the model to Proxima Centauri b

With further advancement of exoplanet detection missions, several Earth-like or rocky, terrestrial exoplanets have already been detected. The closest one to us is that of Proxima Centauri b (PCb), orbiting an M-dwarf star of mass $0.12\,M_\odot$. This system is of particular interest to habitability as the single (officially confirmed) exoplanet is thought to lie within the star's habitable zone where surface liquid water could be sustained. The star's main sequence effective temperature is $T_{\text{eff}} \sim 3050\,\text{K}$ with a current luminosity of $0.15\,L_\odot$ (Anglada-Escudé et al., 2016). The average orbital distance of PCb is 0.0485 AU. Here, we model a hypothetical system, with the Earth scaled to the mass of PCb ($1.27\,M_\oplus$). We initially place the planet at Earth's position in the solar system to distinguish the effects of changing the planetary mass on surface conditions (T_{surf} and P_{CO_2}). Subsequently, the planet is placed at 0.0485 AU from a star of mass $0.12\,M_\odot$, and the evolution of its surface conditions followed up to 20 Gyr, noting that the main sequence lifetime for this star is more than 2000 Gyr, with a current age of ~ 4.8 Gyr (Anglada-Escudé et al., 2016). In this first scenario, the stellar irradiance received on the Earth and the PCb planet is the same. The first results shown in Figure 14 (a) and (b) show the long-term evolution of the surface temperature and atmospheric CO_2 pressure, respectively. Note that the time evolution only extends to 10 Gyr instead of 20 Gyr due to the end of the Sun's main sequence lifetime at this point.

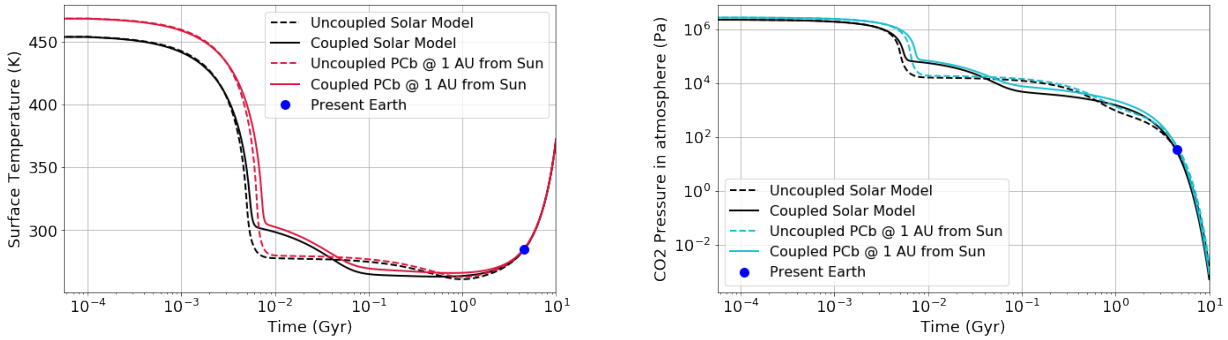

(a) Surface Temperature (K)

(b) Atmospheric CO_2 Pressure (Pa)

Figure 14: Coupled (continuous curve) and uncoupled (dashed curve) evolution of surface conditions for a $1.27\,M_\oplus$ planet (PCb mass) at a distance of 1 AU from the Sun. The blue dot indicates the present-day Earth values of $T_{\text{surf}} = 285\,\text{K}$ and $P_{CO_2} = 33\,\text{Pa}$.

The main feature that can be seen from these results is the initially higher surface temperature on the PCb mass planet in Figure 14a. This is due to the higher planetary mass of $1.27\,M_\oplus$, meaning more radiogenic heating in the mantle and thus a higher initial T_{surf}. This is because a larger planetary mass has an increased volume to surface ratio with respect to the Earth, and thus a hotter mantle due to more radiogenic heating processes taking place. This means a lower mantle viscosity with more convection increasing the mean plate speed. The consequence of this is that there is more CO_2 degassed into the atmosphere by increase

volcanic activity, ultimately leading to higher surface temperatures on the planet via the greenhouse effect. The two models of the Earth and PCb mass planet converge towards the end of the Sun's main sequence lifetime at 10 Gyr due to the significant increase in solar luminosity and subsequent irradiance received. The increasing luminosity plays a larger role at these later evolutionary timescales on the planetary surface conditions than interior processes.

The general trend of the supply-limited weathering regime is similar to the Earth, with a slight time delay for the PCb system due to the higher planetary mass. Both cases for the coupled and uncoupled scenarios obtain very similar values for both the surface temperature and atmospheric CO_2 pressure, ultimately converging at the present-day Earth values of 285 K and 33 Pa respectively, indicated by the blue dots on both figures. This is due to the dominating effects of stellar evolution on these two quantities over the interior evolutionary processes. With a higher surface gravity for PCb due to its larger mass, the weathering rate is the same as on Earth, thus explaining the similar evolution. The initial atmospheric CO_2 pressure in Figure 14b is the same since the reservoir content of CO_2 at $t = 0$ in the atmosphere remains fixed for both models.

Now, we place the PCb-like planet at an observed distance of 0.0485 AU from its host star of mass 0.12 $M_\odot$ to determine how the model quantities of $T_{\rm surf}$ and P_{CO_2} evolve. Here, the model can be extended up to 20 Gyr to take into account the longer main sequence lifetime for the low-mass star. The black curve in Figure 15 indicates the stellar irradiance received by the Earth from the Sun, with a present-day value of 1360 W m^{-2}. The orange curve shows the PCb model, with the red dot indicating the value of PCb of $\sim$ 930 W m^{-2} at 4.8 Gyr.

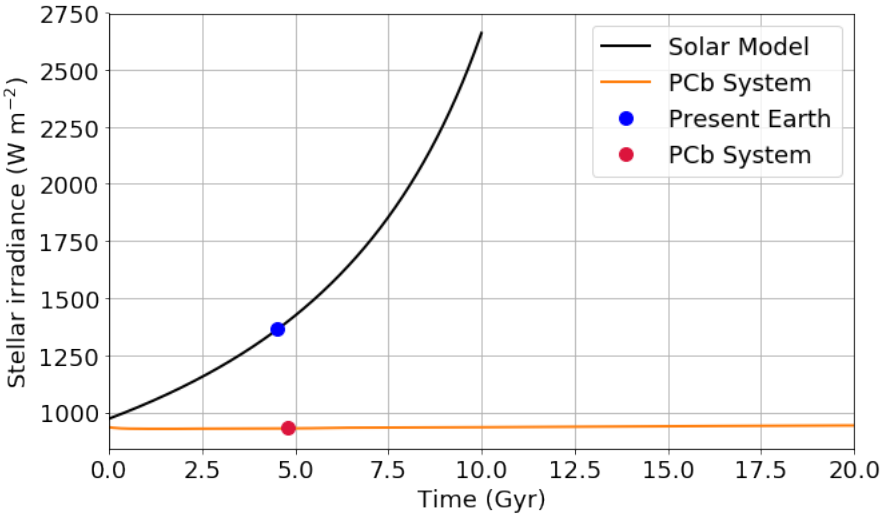

Figure 15: Stellar irradiance for PCb (orange curve) compared to the Earth-Sun model (orange curve). The blue dot indicates the present-day stellar irradiance on Earth of 1360 W m^{-2}. The red dot indicates the value of the PCb system of $\sim$ 930 W m^{-2} at 4.8 Gyr.

Firstly, Figure 15 indicates that the stellar irradiance received by Proxima Centauri b is very

similar to that of the Earth at $t = 0$. PCb experiences a relatively constant stellar irradiation $\sim 930\,\mathrm{W\,m^{-2}}$ for several billions of years, while the Earth's value increases drastically with the earlier end of the Sun's main sequence lifetime. The evolution of T_{surf} and $P_{\mathrm{CO_2}}$ is displayed below in Figure 16 (a) and (b) respectively, again in comparison to the evolution of the Earth and Sun system. Here, the red dots indicate the average values for the PCb system at its current age of $\sim 4.8\,\mathrm{Gyr}$, with $T_{\mathrm{surf}} = 255\,\mathrm{K}$ and $P_{\mathrm{CO_2}} = 2500\,\mathrm{Pa}$. Similar to before, the blue dots indicate the present-day average values on Earth.

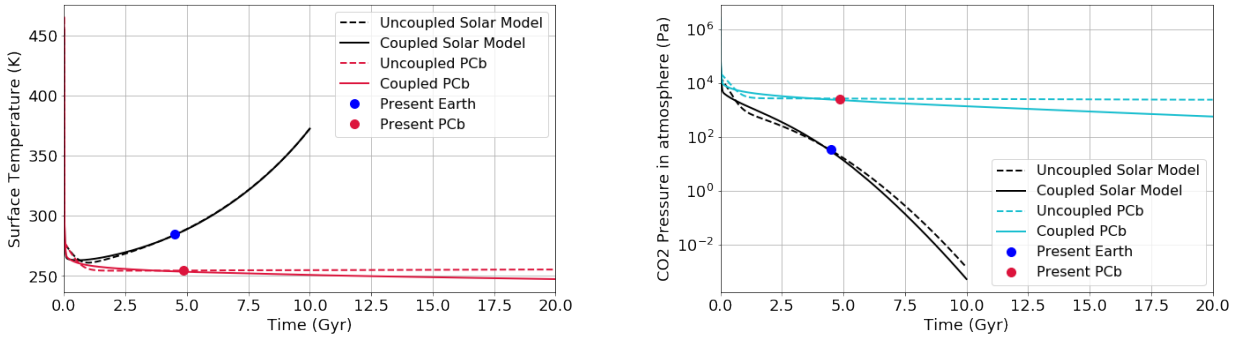

(a) Surface Temperature (K)

(b) Atmospheric CO_2 Pressure (Pa)

Figure 16: 20 Gyr evolution for coupled (continuous curves) and uncoupled (dashed curves) model of surface condition for PCb (red and blue curves) compared to the Earth-Sun model (black curves), with blue dot indicating present-day Earth value of $T_{\mathrm{surf}} = 285\,\mathrm{K}$ and $P_{\mathrm{CO_2}} = 0.33\,\mathrm{Pa}$. The red dots indicate the PCb value of $T_{\mathrm{surf}} = 255\,\mathrm{K}$ and $P_{\mathrm{CO_2}} = 2500\,\mathrm{Pa}$ at $4.8\,\mathrm{Gyr}$.

The evolution of the surface temperature for PCb, from Figure 16b can be seen to be much lower and constant than for the Earth. This does not provide habitable conditions however as the $T_{\mathrm{surf}} \sim 250\,\mathrm{K}$ for both the coupled and uncoupled models, below the habitability condition resulting in a permanently glaciated planet. Even though the $P_{\mathrm{CO_2}}$ for both the Earth and the PCb planet start off at almost the same value, the exoplanet retains a higher value for a longer period of time compared to the Earth. Additionally, the CO_2 pressure does not decline as drastically as for the Earth, but rather remains relatively stable between $P_{\mathrm{CO_2}} \sim 10^4 - 10^2\,\mathrm{Pa}$ for up to, and most likely beyond, $20\,\mathrm{Gyr}$ due to the longer main sequence lifetime of its low mass central star. For these surface conditions on the PCb-like planet, the consequences of frozen surface water is that the carbon cycle cannot function as the climate stabilizing mechanism necessary to sustain habitable conditions.

All in all, this system could have been considered habitable in the past, when warmer temperatures could have supported the existence of liquid water and thus carbon-based life such as on Earth. However, the present-day freezing temperatures, likely to be maintained for several billions of years, do not seem promising for habitability without taking into account extremophile species.

5 Discussion

With the continuous advancement of exoplanet detection missions, more rocky and terrestrial planets could be discovered to have similar properties as the Earth. Some of the most likely candidates are the low-mass M-dwarf stars for their abundance in our galaxy, as well as long main sequence lifetimes and corresponding stable luminosities. In order to determine whether an exoplanet is habitable, it must be within the habitable range where surface liquid water could be sustained on geologic timescales ($\geqslant 10^7$ Myr). The surface temperature of a planet is regulated by the negative feedback mechanism of the carbon cycle via the atmospheric CO_2 pressure and greenhouse effect. Throughout this work, we have considered two cases of an uncoupled or coupled model for an Earth-like planet, although the precise thermal evolution of the Earth is still a source of debate. This could, therefore, present as a source of uncertainty in our results. However, it has been determined that these interior effects are primarily important in the first few million years of planetary evolution, and are not as relevant on longer timescales beyond 1 Gyr.

An online tool for determining the habitable zone of main sequence stars can be used as an estimator for various types of stars. This is based on the work of Kopparapu, Ramirez, Kasting, et al. (2013) and Kopparapu, Ramirez, Schottel, et al. (2014). In this model, the two input parameters are the stellar effective temperature and the luminosity (in solar units). The outputs are two sets of distances defining the habitable zone, either the conservative limits considering the inner habitable zone of the moist greenhouse limit, similar to the runaway greenhouse, and the outer with the maximum greenhouse limit. This model is based on a 1D radiative-convective, cloud-free climate model, which can be applied to F, G, K and M type stars (Kopparapu, Ramirez, Kasting, et al., 2013). The stellar irradiance on the surface of a planet is deemed to be the most important quantity in determining the potential habitability. This means that there is no dependence on the albedo (or reflectivity) of the planet, which can vary for different surface compositions and wavelength of starlight received (Kopparapu, Ramirez, Kasting, et al., 2013). One effect not included in their model is that of clouds, and thus it is possible that their habitable zone limits could be extended (quite significantly) in both directions. For both the inner and outer habitable zone calculations, an 'inverse climate model' is used, meaning that with a certain planetary surface temperature, the flux, and thus distance to the star, is calculated in order to sustain habitable conditions. The standard metric used is that of the Earth-Sun system, and so the flux incident on the top of the planet's atmosphere is taken to be the same as the present-day Earth.

The habitable zone ranges determined by the estimator can be compared to the results of our model for the same stellar types. It is important to note that the estimator habitable zone is determined by the moist greenhouse (~ 340 K) and maximum greenhouse limits (~ 250 K), slightly different to our habitable conditions of the freezing point of water (273 K) and an upper limit of 343 K considering the degradation of proteins necessary for photosynthesis. For a $0.1\,M_\odot$ star with effective temperature 2800 K and luminosity of $L/L_\odot \approx 0.001$, the estimator habitable zone limits are $0.033-0.066$ AU, significantly wider than the estimate ob-

tained from our model of $\sim 0.023 - 0.0029$ AU. The same comparison between the estimator and our uncoupled model was made for the $0.5\,M_\odot$ star with a stellar effective temperature of 3660 K, luminosity of $L/L_\odot \sim 0.0407$. The estimator limits for this type of star are $0.209 - 0.402$ AU, again, significantly higher and wider than our range of $0.175 - 0.223$ AU. Their model does not take into account interior planetary processes as our model does, with the two cases for the coupled or uncoupled thermal evolution of the mantle to the carbon cycle, although these two cases are only relevant for the initial planetary evolution up to ~ 1 Gyr, and the long term P_{CO_2} evolution, as demonstrated in section 4.2. Both models are albedo-independent as the stellar irradiance is taken to be a wavelength integrated quantity.

In terms of habitability around low-mass stars, the stellar flares most prevalent in the first 1 Gyr of M-dwarf lifetimes (Scalo et al., 2007). These can potentially be lethal, especially since the distance from the star at which an exoplanet can receive enough stellar irradiance for habitable surface temperatures and potential for liquid water is very close, with average distances less than 0.1 AU. However, after this initial stage, and once the star settles onto the main sequence, its luminosity does not increase significantly for several billion years, which could benefit long-term habitability. These timescales of stable (or slightly increasing) luminosity far surpass the habitable limit for the Earth, considering the increasing luminosity of the Sun before its red-giant phase at 10 Gyr. Another important effect to consider is that of tidal locking. Tidal locking was previously believed to cause an atmospheric freeze-out on the side not irradiated by the star, and excessive amounts of radiation received on the other (Tarter et al., 2007). Additionally, the magnetic field intensity of a tidally locked planet can be significantly reduced, exposing the surface to further XUV radiation from the star (Scalo et al., 2007). Altogether, tidally locked planets should not be excluded as habitable candidates, although it remains a topic of debate.

One parameter which can greatly influence the location of the habitable zone around a low-mass star is the planetary albedo, A, which determines the amount of stellar radiation reflected from the surface of the planet. We kept $A = 0.31$ based on the present-day Earth average value, however, this would be higher for planets with more ice cover being more reflective (James Kasting, Whitmire, and Reynolds, 1993). As we are considering low-mass stars with lower effective temperatures than the Sun, their peak wavelength emission is shifted towards the infrared. This is significant for the albedo effect since longer wavelengths significantly increase the absorption coefficients of H_2O and CO_2 with respect to the visible wavelength ranges (James Kasting, Whitmire, and Reynolds, 1993). This means that for an Earth-like planet orbiting a cooler, red star, more of its starlight is absorbed by its atmosphere with respect to a hotter, more blue star. This effect becomes even more pronounced for high concentrations of atmospheric greenhouse gases (high P_{CO_2}) (James Kasting, Whitmire, and Reynolds, 1993). These changes in the albedo can significantly alter the boundaries of the inner and outer habitable zone, by as much as 30%, depending on the stellar system (James Kasting, Whitmire, and Reynolds, 1993). This would mean that if a planet is initially considered to be too cold to host life, by considering a lower value of the albedo, the planet could migrate into the habitable zone by appearing as if it were closer to the star compared to when it had the same value of the albedo as the Earth. The albedo can also be considered as a positive feedback which aids the runaway ice-house effect and destabilizing

the climate on a planet (James Kasting, Whitmire, and Reynolds, 1993). Furthermore, it has not been explored in this work how various greenhouse gases, most importantly CO_2 and H_2O, are affected by different wavelengths of stellar radiation.

Throughout this work, we maintained an offset of 1 Gyr between the stellar and planetary evolution models, such that the planet begins its fully-formed evolution during the main-sequence phase of the central star. However, other timescales could be considered taking into account more precise planet formation and evolutionary timescales around these low-mass stellar systems. This offset, if altered by $\gtrsim 0.1$ Gyr, can significantly influence the position of the habitable zone, since the stellar luminosity is much higher during the pre-main sequence phase of such systems.

6 Conclusion

Due to the abundance of low-mass stars in the Milky Way, we should investigate whether they are likely candidates to host extraterrestrial life. By considering an Earth-like planet in a close orbit to these stars, the long-term evolution of interior (planetary) and exterior (stellar) processes can help to determine potential habitable conditions based on the surface temperature T_{surf} and atmospheric CO_2 pressure P_{CO_2}. On Earth, the carbon cycle is necessary for stabilizing the climate via the greenhouse effect over geologic timescales. By adapting the planetary evolution and carbon cycle model of Oosterloo (2020), we were able to find the long-term evolution of T_{surf} and P_{CO_2}, on Earth-like exoplanets around stars of mass $0.1\,M_\odot$ and $0.5\,M_\odot$ for up to 20 Gyr.

We initially modeled the same value of the solar irradiance at $t = 0$ as the Earth for both exoplanet systems, positioning them at circumstellar distances of 0.0342 AU and 0.247 AU from the $0.1\,M_\odot$ and $0.5\,M_\odot$ stars respectively. From these results, it was possible to determine that stellar evolution begins to play the dominating role in influencing both the surface conditions (T_{surf} and P_{CO_2}) at ~ 0.1 Gyr. Before this, both for the coupled and uncoupled scenarios, the planets experience exactly the same surface conditions as the Earth due to the same interior processes. As the Earth's surface temperature begins to increase at 1 Gyr due to the increasing luminosity of the Sun, more significant towards the ends of its main sequence lifetime, surface temperatures will surpass the habitable limit of 343 K before 10 Gyr. The modeled exoplanet systems are also not deemed habitable as the surface temperatures are too close to, or even below, the freezing point of water at ~ 1 Gyr. These low temperatures, sustained for several billions of years, result in a permanently glaciated and possibly uninhabitable planet. Even with the relatively high values of P_{CO_2} for several billions of years, the carbon cycle is not able to regulate the climate due to a lack of surface liquid water.

A habitable range of surface conditions was determined by modelling various orbital distances of the Earth-like exoplanet to the low-mass central star. The habitability of these systems is based on the potential for liquid water to exist, and thus the temperature range must lie within the freezing point of water, and an upper limit of 343 K set as a biological limit for the degradation of proteins necessary for photosynthesis (Rushby et al., 2018). From these models, it can be seen that for a $0.1\,M_\odot$ star, the habitable range of distances lies between $0.024 - 0.0280$ AU, with the inner limit valid for the uncoupled model. After the initial equilibrium period of $\sim 10^{-2}$ Gyr, the long-term temperature range at these distances lies between $290 - 330$ K, while the corresponding long-term P_{CO_2} changes by several orders of magnitude, from a maximum of 10^4 to 0.1 Pa, respectively. For the case of the $0.5\,M_\odot$ star, the habitable range of distances is larger, from $d = 0.180$ to 0.220 AU with the same surface temperature range. The atmospheric CO_2 pressure for these distances corresponds to $\sim 10^2 - 0.1$ Pa, although a large difference of one order of magnitude can be observed. These indicate promising conditions for the long-term evolution of life, but the boundaries could still be modified by alterations in the model such as including the albedo effect and taking into account effects of tidal locking or stellar flares, as discussed in section 5. If

different habitable zone limits are considered, such as the moist greenhouse at $T_{\text{surf}} \gtrsim 340\,\text{K}$ or a lower bound of 248 K for which all surface water would be permanently frozen in a few thousand years, then the inner and outer habitable zone limits could be slightly extended in both directions.

Finally, we applied the model to the hypothetical system of Proxima Centauri b, by changing the planetary mass, stellar mass, and orbital distance in the model. These results show several initially promising features, such as the remarkably similar stellar irradiance received in the first few million years in comparison to the Earth. Additionally, the surface temperature of the exoplanet shows very similar trends to the Earth, only deviating after one billion years due to the difference in stellar evolution of the two models (due to the longer main sequence lifetime of the lower mass star). However, the planet appears to be permanently frozen on billion-year timescales, and is thus not considered habitable.

Overall, it has been calculated that habitable surface conditions can be maintained for long periods of time (up to and most likely extending beyond 20 Gyr) on Earth-like planets orbiting stars of lower mass than the Sun. If effects such as tidal locking and stellar flares are not considered, then these stars can be seen as excellent candidates for life to survive and evolve for long periods of time, due to the longer main sequence lifetime of their low-mass stars which maintain a relatively constant luminosity over billions of years. The carbon cycle can therefore be considered an efficient mechanism in retaining habitable surface conditions based on T_{surf} and P_{CO_2}, given that these quantities do not surpass the limits of habitability. If they do, this could induce a permanent global glaciation for temperatures below the freezing point of water, or complete evaporation of all surface water for temperatures above the runaway greenhouse limit. The habitable zone limits considered in our model applies to clement conditions for life, thus a narrower habitable zone range around these low-mass stars is found with respect to other models.

References

Adams, F, P Bodenheimer, and G Laughlin (2005). "M dwarfs: planet formation and long term evolution". In: *Astronomische Nachrichten: Astronomical Notes* 326.10, pp. 913–919.

Anglada-Escudé, Guillem et al. (2016). "A terrestrial planet candidate in a temperate orbit around Proxima Centauri". In: *Nature* 536.7617, pp. 437–440.

Christensen-Dalsgaard, Jørgen (2021). "Solar structure and evolution". In: *Living Reviews in Solar Physics* 18.1, pp. 1–189.

Foley, Bradford (2015). "The role of plate tectonic-climate coupling and exposed land area in the development of habitable climates on rocky planets". In: *The Astrophysical Journal* 812.1, p. 36.

Gaidos, E et al. (2016). "They are small worlds after all: revised properties of Kepler M dwarf stars and their planets". In: *Monthly Notices of the Royal Astronomical Society* 457.3, pp. 2877–2899.

Gough, DO (1981). "Solar interior structure and luminosity variations". In: pp. 21–34.

Hansen, Carl and Steven Kawaler (1994). *Stellar Interiors: Physical Principles, Structure, and Evolution*. Springer-Verlag.

Kasting, James, Daniel Whitmire, and Ray Reynolds (1993). "Habitable zones around main sequence stars". In: *Icarus* 101.1, pp. 108–128.

Kopparapu, Kumar (2013). "A revised estimate of the occurrence rate of terrestrial planets in the habitable zones around Kepler M-dwarfs". In: *The Astrophysical Journal Letters* 767.1, p. L8.

Kopparapu, Kumar, Ramses Ramirez, J Kasting, et al. (2013). "Habitable zones around main-sequence stars: new estimates". In: *The Astrophysical Journal* 765.2, p. 131.

Kopparapu, Kumar, Ramses Ramirez, James Schottel, et al. (2014). "Habitable zones around main-sequence stars: dependence on planetary mass". In: *The Astrophysical Journal Letters* 787.2, p. L29.

LeBlanc, Francis (2011). *An introduction to stellar astrophysics*. John Wiley & Sons.

Lehmer, Owen, David Catling, and Joshua Krissansen-Totton (2020). "Carbonate-silicate cycle predictions of Earth-like planetary climates and testing the habitable zone concept". In: *Nature communications* 11.1, pp. 1–10.

Lissauer, Jack J (Sept. 2018). *Habitable zone*. URL: `https://www.britannica.com/science/habitable-zone`.

Mamajek, Eric (Mar. 2021). *A Modern Mean Dwarf Stellar Color and Effective Temperature Sequence*. URL: `http://www.pas.rochester.edu/~emamajek/EEM_dwarf_UBVIJHK_colors_Teff.txt`.

Oosterloo, Mark (2020). *The role of plate tectonics in the long-term evolution of atmospheric carbon dioxide content on Earth-like exoplanets*.

Perryman, Michael (2018). *The exoplanet handbook*. Cambridge University Press.

Pierrehumbert, Raymond T (2009). *Principles of Planetary Climate*. Cambridge University Press.

Rushby, Andrew J et al. (2018). "Long-term planetary habitability and the carbonate-silicate cycle". In: *Astrobiology* 18.5, pp. 469–480.

Safonova, Margarita et al. (2021). "Quantifying the Classification of Exoplanets: in Search for the Right Habitability Metric". In: *arXiv preprint arXiv:2104.02991*.

Scalo, John et al. (2007). "M stars as targets for terrestrial exoplanet searches and biosignature detection". In: *Astrobiology* 7.1, pp. 85–166.

Schubert, Gerald, Donald Turcotte, and Peter Olson (2001). *Mantle convection in the Earth and planets*. Cambridge University Press.

Shields, Aomawa L, Sarah Ballard, and John Asher Johnson (2016). "The habitability of planets orbiting M-dwarf stars". In: *Physics Reports* 663, pp. 1–38.

Siess, Lionel, Emmanuel Dufour, and Manuel Forestini (2000). "An Internet server for update pre-main sequence tracks of low-and intermediate-mass stars". In: *arXiv preprint astro-ph/0003477*.

Sleep, Norman H and Kevin Zahnle (2001). "Carbon dioxide cycling and implications for climate on ancient Earth". In: *Journal of Geophysical Research: Planets* 106.E1, pp. 1373–1399.

Tarter, Jill C et al. (2007). "A reappraisal of the habitability of planets around M dwarf stars". In: *Astrobiology* 7.1, pp. 30–65.

Walker, J, P Hays, and J Kasting (1981). "A negative feedback mechanism for the long-term stabilization of Earth's surface temperature". In: *Journal of Geophysical Research: Oceans* 86.C10, pp. 9776–9782.

Wolf, Eric et al. (2017). "Constraints on climate and habitability for Earth-like exoplanets determined from a general circulation model". In: *The Astrophysical Journal* 837.2, p. 107.